Environmental Science
Water Research & Technology

Low-Cost Desalination for Seawater and Hybersaline Brine Using Nanophotonics Enhanced Solar Energy Membrane Distillation

Journal:	*Environmental Science: Water Research & Technology*
Manuscript ID	EW-ART-03-2020-000254.R1
Article Type:	Paper

WATER IMPACT STATEMENT

The presented technology of Nanophotonics Enhanced Solar Membrane Distillation (NESMD) introduces a low-cost high-efficiency solution for desalination of seawater and hypersaline brine using only solar energy. The NESMD implements nanophotonic materials on a commercial hydrophobic membrane. The photothermal coating serves as a solar-thermal collector, absorbs solar energy, and generates highly localized heat on the membrane.

Low-Cost Desalination for Seawater and Hybersaline Brine Using Nanophotonics Enhanced Solar Energy Membrane Distillation

Ibrahim A. Said[1,2*], Naomi Fuentes[1], Ze He[2], Ruikun Xin[1, 2], Kuichang Zuo[1,2], Qilin Li[1, 2*]

[1]Nanotechnoly-Enabled Water Treatment Center (NEWT), Rice University, MS 6398, 6100 Main Street, Houston 77005, United States

[2]Department of Civil and Environmental Engineering, Rice University, MS 519, 6100 Main Street, Houston 77005, United States

*Corresponding author: dr.ibrahim.a.said@gmail.com (I.A.S) & Qilin.li@rice.edu (Q.L.)

Abstract

A stand-alone small-scale Nanophotonics Enhanced Solar Membrane Distillation (NESMD) testbed was designed, developed, and tested for desalinating seawater and high salinity feedwaters. This NESMD system can take almost any source water, and turn it into clean water with sunlight as the only energy source. The NESMD technology applies nanophotonic coating materials on commercial hydrophobic Polypropylene support of a Polytetrafluoroethylene (PTFE) membrane surface. The photothermal coating serves as a solar-thermal collector, absorbs solar energy, and generates highly localized heat on the membrane, while the rest of the membrane performs the membrane distillation function. The presented NESMD system is equipped with an internal heat recovery system with no need for external electricity and no additional water for cooling. The NESMD testbed is installed and tested at Rice University campus (29.7174° N, 95.4018° W). In this study, real seawater from Galveston Bay, Texas U.S., and high salinity simulated feedwaters (total dissolved solids (TDS) 113,200– 200,000 PPM) have been tested for long-term testing in the weather conditions of Houston, Texas. The field testing results showed a stable desalination performance in consecutive 5-8 hour operation cycles, with TDS removal ≥ 99.5% in all experiments. Average daily membrane flux of ≥ 0.75 L/m^2-hr was achieved at a solar intensity close to 1 kW/m^2 without external heat exchanger. Further investigations and improvements are required to enhance the performance of the reactor since it is still a new promising technology.

Keywords

Nanophotonics; photothermal coating; solar energy; desalination; membrane flux

1. Introduction

Increasing population, global climate change, and continuing industrial contamination of freshwater sources impose increasing demand on water supply. Utilizing alternative water sources including brackish water, seawater, wastewater, oil and gas produced waters, and other impaired or currently, unusable water sources is an important strategy to meet current and future water needs and to prepare our societies to the uncertainties in water resources caused by global climate change. A critical need in treating these alternative water sources is desalination. Conventional thermal processes, e.g., multistage evaporation (MSE) and multi-effect distillation (MED), and membrane-based desalination, i.e., reverse osmosis (RO) and nanofiltration (NF), have been successfully applied at various scales to desalinate and purify a wide range of source waters[1, 2]. In 2017, 99.8 $\times 10^6$ m^3/day of freshwater was produced by desalination plants worldwide[3]. In particular, membrane-based desalination systems have seen a steady increase in installed capacity in the past few decades[4]. However, desalination is a high energy-intensive process. Reverse osmosis (RO) consumes 1.5 to 2.5 kWh/m^3 to desalinate seawater[5]; it requires significant capital investment and extensive pretreatment to control membrane fouling and scaling. Also, water recovery of RO desalination systems is between 50 and 85%, leaving large volumes of concentrated brine.

For desalination plants that are located away from the coastal line, disposal of the RO brine poses a major challenge and is very costly. Furthermore, a big challenge is coming up to the water communities is the produced water from the oil and gas industries. The produced water is a term frequently used to describe wastewater generated during the extraction of fossil fuels from geologic formations. Currently, the output of produced water exceeds oil production at a volumetric ratio of 3:1 globally [6-9]. These large volumes of wastewater have been projected to increase in the near future with higher total dissolved solids, particularly in the US, where the advent of horizontal drilling and hydraulic fracturing of unconventional formations has led to the Shale Revolution [10-13]. Throughout the 30-year lifetime of a well, the water-to-oil ratio increases [6, 13, 14], making produced water, without doubt, the largest waste stream emanating from the oil and gas industry.

Novel desalination methods that use less energy and recover more water are greatly needed to improve the economic feasibility of desalinated water as water supplies as well as treating high salinity waters from oil and gas produced waters. A promising approach to reduce the energy consumption of desalination is to use renewable energy. Authors propose a novel, nanophotonics

enhanced direct solar membrane distillation process to treat real seawater and high-salinity simulated feed waters using sunlight. The proposed process efficiently uses sunlight instead of electricity from the power grid or solar photovoltaic panels to drive membrane distillation. It has the benefit of conventional membrane distillation (MD) processes [15-35] i.e., low pressure, low fouling potential, insensitive to total dissolved solids (TDS) concentration, and potential for zero liquid discharge, but with greatly enhanced energy efficiency.

In a NESMD system, the active surface of the membrane on the feed side is exposed to sunlight through the transparent membrane housing of plate-and-frame configuration; the membrane serves both as the solar thermal collector and the hydrophobic barrier between the feed and permeate. It overcomes several critical limitations of existing solar MD technologies responsible for their low solar thermal efficiency. First, the nanomaterials used are highly efficient photothermal converters, and the photothermal coating heats the feed water directly in the MD module without the need for heat exchangers. Second, light is optically trapped in a thin porous coating, resulting in a high heating intensity and therefore high temperature on the membrane surface. More details about the NESMD system can be found elsewhere[36].

A small scale NESMD system of 0.2 m^2 as an active membrane surface area was designed, developed, and tested to generate benchmark process data and design parameters needed for designing a large NESMD system and commercialization. The overall objective of the NESMD activities was the development of a stand-alone desalination testbed with low maintenance needs for remote areas with a lack of drinkable water but have seawater with high solar irradiation. Furthermore, high-salinity simulated feed water, which is a major concern from the oil and gas produced waters, will be tested via the NESMD system.

In the current study, authors have evaluated the potential of the NESMD technology for the treatment of real seawater from Galveston Bay, Galveston, Texas U.S.. Also, the NEMSD has tested using high salinity simulated feed waters (TDS of 113,200, 121,700, 139,800, 172,600, and 200,000 PPM). All the experiments have been executed outdoor taking into consideration the weather conditions of Houston, Texas.

2. Experiments

2.1 Nanophotonics Enhanced Solar Energy Membrane Preparation

The NESMD is a unique bilayer nanostructure consisting of a solar-absorbing, hydrophilic, carbon black nanoparticle-infused polypropylene (PP) layer, overlying a microporous hydrophobic layer of polytetrafluoroethylene (PTFE). The uncoated PTFE membrane has an average porosity of 77%, an average pore size of 0.2-μm, and an average thickness of 218.23 μm with the supporting PP layer accounting for 84.5% of the total thickness (Figure 1). The uncoated PTFE membrane also showed excellent hydrophobicity with a Liquid Entry Pressure (LEP) of 317.2 kPa for water, and water contact angle measurements averaging 153.2 (± 2.3^{o}) and 157.1 (± 1.7^{o}) for PTFE and PP, respectively. The NESMD membrane is prepared by directly coating functionalized carbon black nanoparticles (Cobalt Corporation) on the PP layer of the commercial hydrophobic PTFE membrane (Pall Corporation). Two different solutions; the polydopamine (PD) solution and the carbon black (CB) solution have been used for preparing the NESMD membrane. The two solutions were concocted in 50-mL, polypropylene conical tubes (Corning® CentriStar, Fisher Scientific) and utilized a 3:2 volumetric ratio of ethanol-water as the solvent in each respective solution. The preparation process started by applying a polydopamine adhesion layer to the PP side followed by a second coating of carbon black nanoparticles. Due to the larger pore size of the PP support layer relative to the 0.2-μm PTFE layer, the solvent was able to penetrate, or wet, the PP layer, thus making it hydrophilic, without wetting the PTFE layer. More details regarding the preparation of the photothermal coating can be found elsewhere[37-39]. Figure 1 shows SEM images of the NESMD photothermal coating on the surface of the PP layer. The SEM images in Figure 2 show a successful photothermal coating of the nanophotonics materials on the surface of the hydrophobic PP of the PTFE membrane.

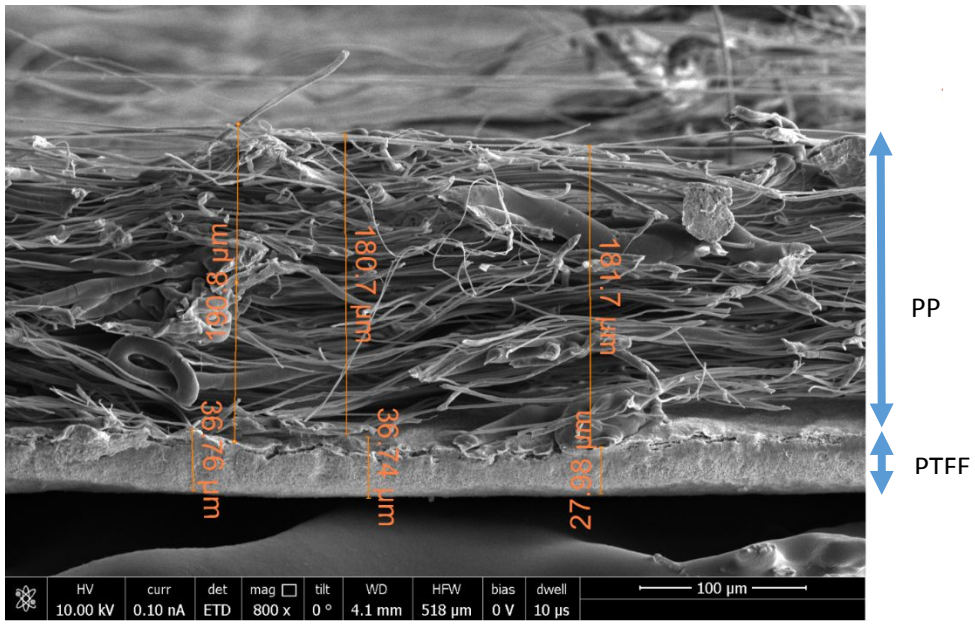

Figure 1. A cross-sectional view of the uncoated PTFE/PP membrane

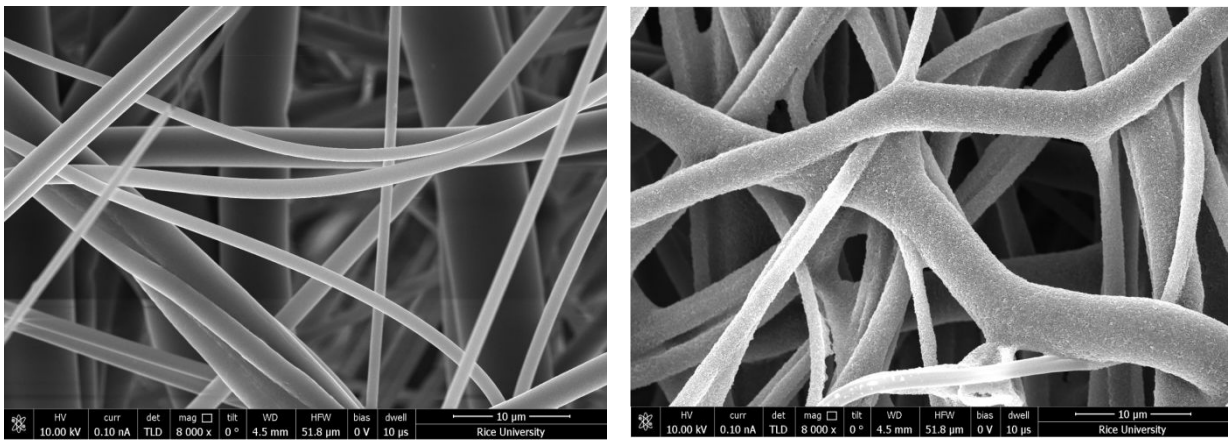

Figure 2. SEM surface images of (left) uncoated PP of PTFE membrane, (right) nanophotonics coating of PP layer (10 µm Resolution)

2.2 Sweeping Gas Membrane Distillation (SGMD): Operation Mode

An SGMD operational mode has been used in the current NESMD experiments [40]. The SGMD is similar to air gap membrane distillation (AGMD)[41], but instead of a stagnant gap of air on the permeate side, a flow of cold air flowing underneath the membrane to sweep off and collect the permeate. The SGMD advantages address primary issues with other MD modes.

The reduction of heat transfer via conduction, and reduced resistance to mass transfer as a result of the flow of gas on the permeate side and a low risk of pore wetting highlight the potential of SGMD and make it an attractive area of research & development.

3. Experimental Prototype Description

3.1 NESMD Prototype: Design and Development

A three-channel plate and frame NESMD reactor with an effective membrane surface area of 0.2 m^2 (0.25 x 0.9 m) has been designed, developed, and built to house the nanophotonics solar membrane. Figure 3 shows a schematic diagram of the NESMD system and a physical picture of the NESMD reactor. The membrane module consists of three flow channels: 1) the coolant (bottom) channel where the cold feedwater exchange heat with the vapor in the sweeping air (middle) channel to condense the vapor and gets heated itself; 2) a feed (top) channel formed between a transparent window and the photothermal membrane, where the preheated feedwater evaporates at the feed-membrane interface and the vapor transports through the membrane; and 3) the sweeping air channel, where the vapor is contacted with a heat exchange surface and condenses. Figure 4 shows the design of the different components of the NESMD membrane module that form the flow channels.

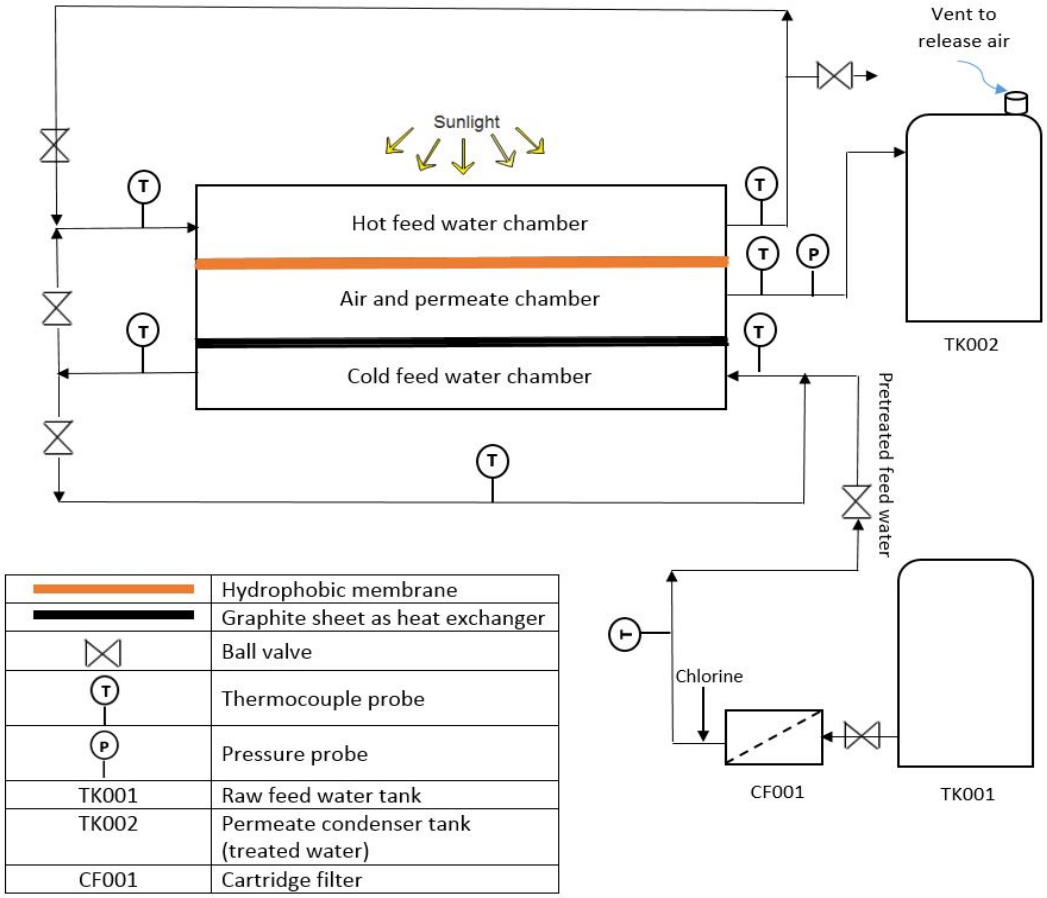

	Hydrophobic membrane
	Graphite sheet as heat exchanger
	Ball valve
T	Thermocouple probe
P	Pressure probe
TK001	Raw feed water tank
TK002	Permeate condenser tank (treated water)
CF001	Cartridge filter

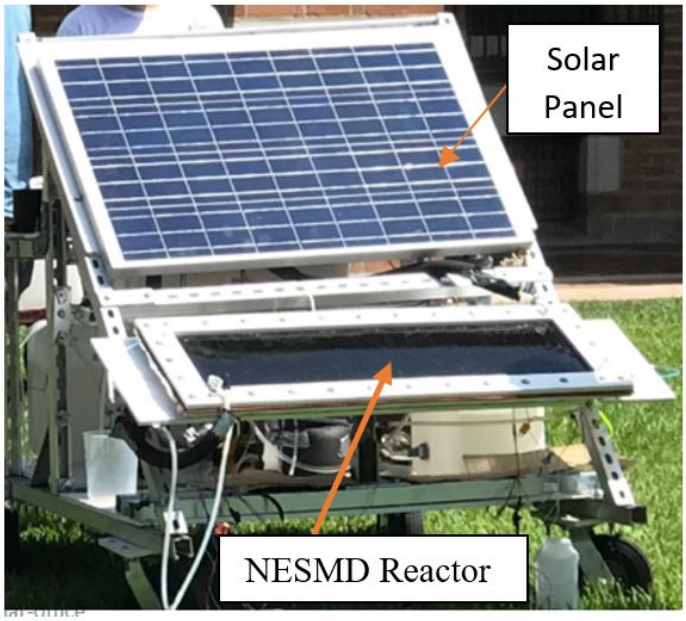

Figure 3. Schematic diagram of the NESMD prototype and physical picture of the NESMD system

A and I	Acrylic closing plates (thickness 12.7 mm)
B	Irradiation acrylic glass (thickness 3mm)
C,E, and G	Silicon rubber frames
D	Hydrophobic membrane
F and H	Plastic net spacer
1	Inlet hot feed water
2	Outlet hot feed water
3	Inlet cold feed water
4 = 1	Outlet cold feed water, which is the inlet of feed water
5	Distillate
6	Venting line

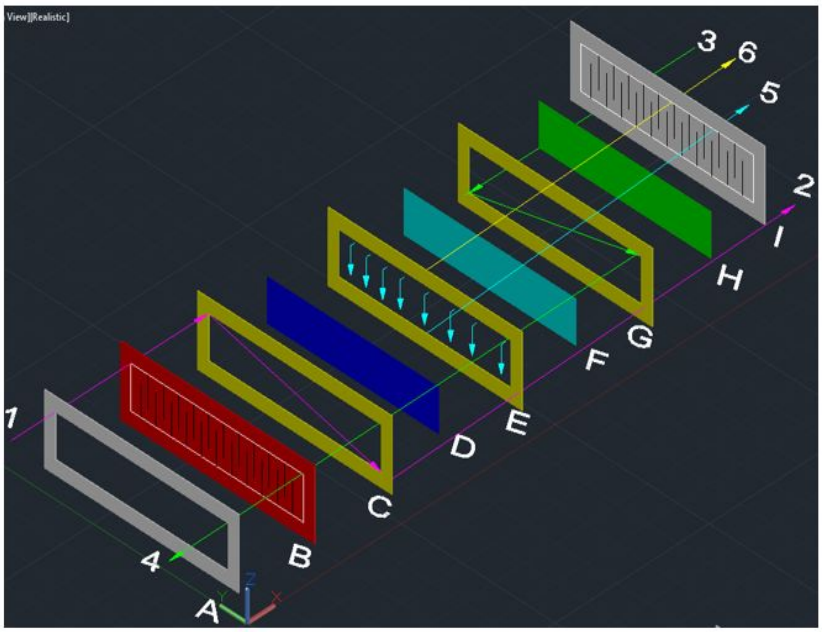

Figure 4. Main components of the membrane configuration of NESMD

Hydraulic conditions in each of the flow channels are very important to the performance of the reactor. They not only determine the contact time each flow stream has for evaporation, heat exchange or condensation, but also strongly affect the mass and heat transfer. In the current design, the top and bottom flow chambers are equipped with built-in flow baffles to achieve uniform fluid distribution, while the middle chamber will be filled with a woven mesh spacer. Figure 5 shows AutoCAD drawings for detailed drawings for all designed components of the membrane module. The three flow channels are generated by two high-density polyethylene (HDPE) with UV resistance closure plates, Plexiglas acrylic as transmittance window, gasket materials, and a microporous photothermal membrane with an average pore size of 0.2 μm on supported polypropylene support.

Material selection procedures (Figures 6) was performed to choose the right materials for the reactor. On the light of the material section diagram, the transmittance window was made of clear Plexiglas of 92% light transmission. The Plexiglas acrylic is crystal clear, colorless, high

impact resistance, low water absorption, and corrosion and chemical resistance. While the closure plates were made of high-density polyethylene with UV resistance. The reasons for selecting the HDPE with UV resistance were mainly about its outstanding weatherability, lightweight, and corrosion, and chemical resistance.

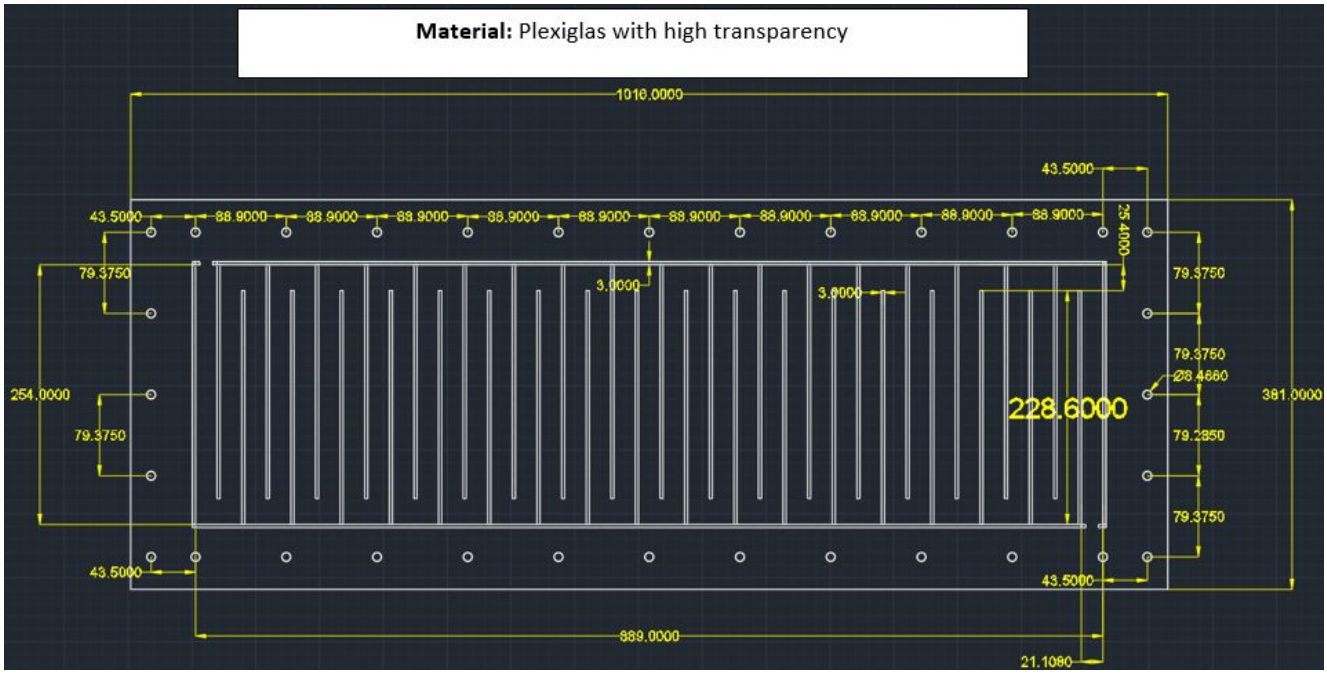

a. Transmittance Sheet (all dimensions are in mm)

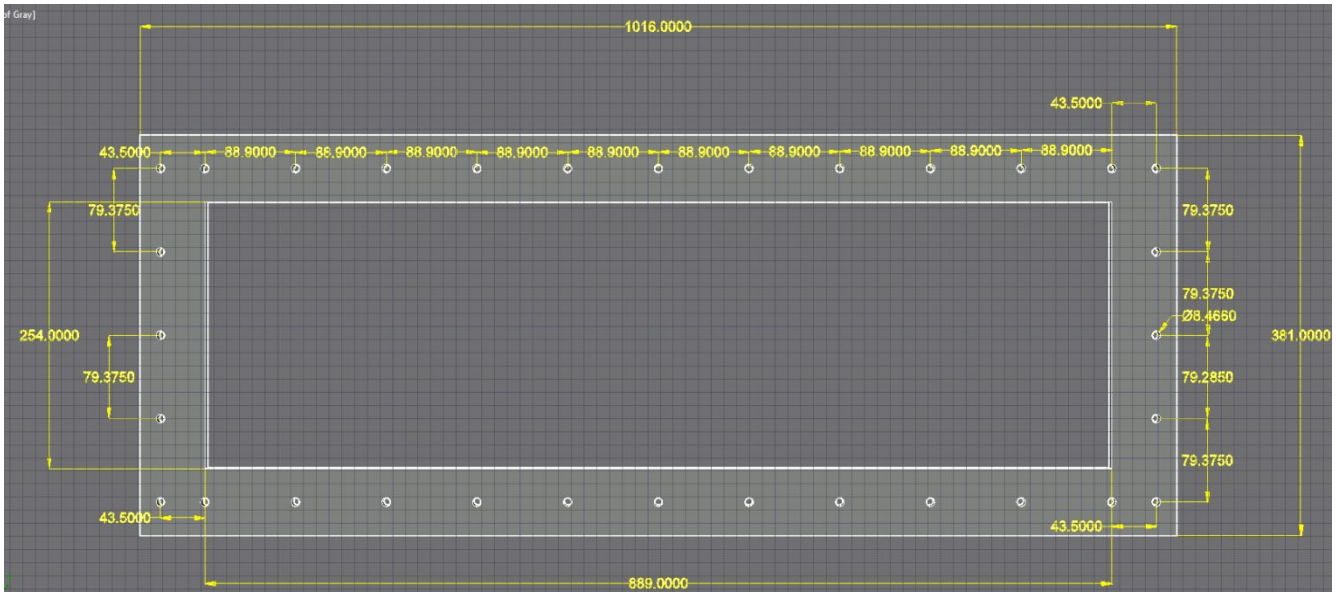

b. Top closure plate (all dimensions are in mm)

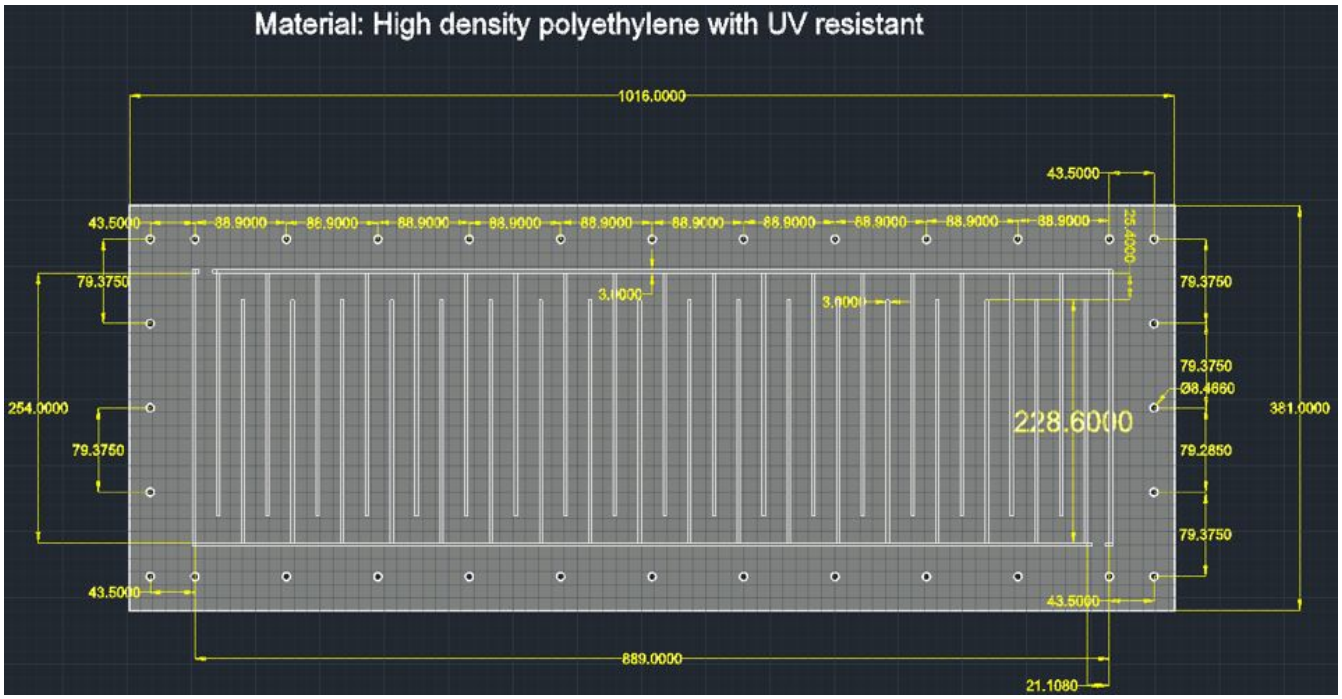

c. Top view of the bottom closure plate (all dimensions are in mm)

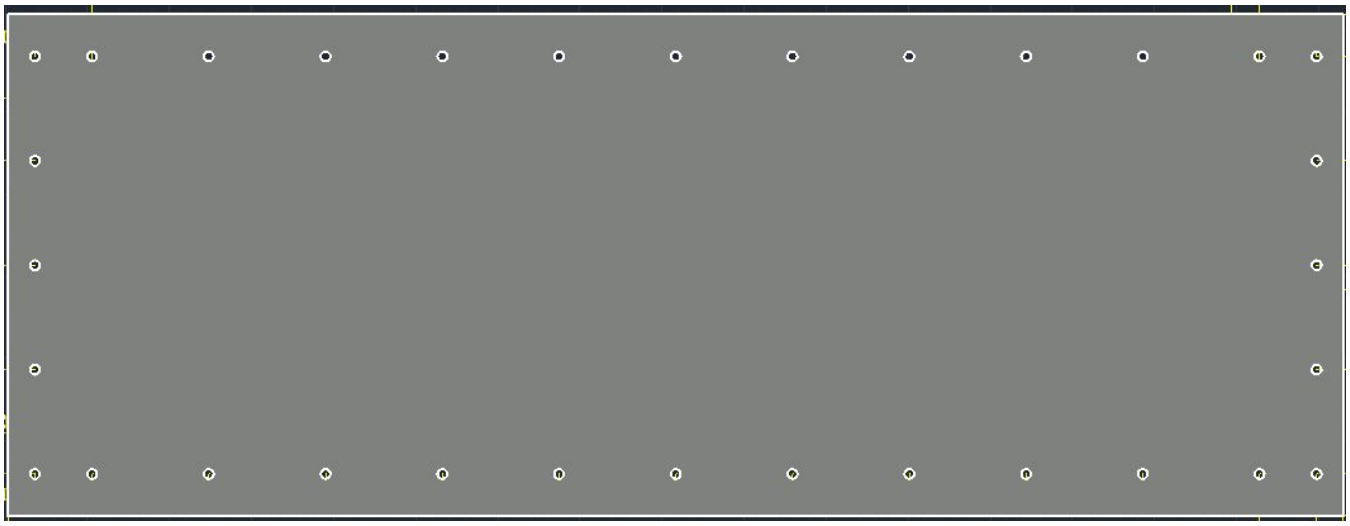

d. Bottom view of the bottom closure plate

Figure 5. AutoCAD design drawings of NESMD reactor components.

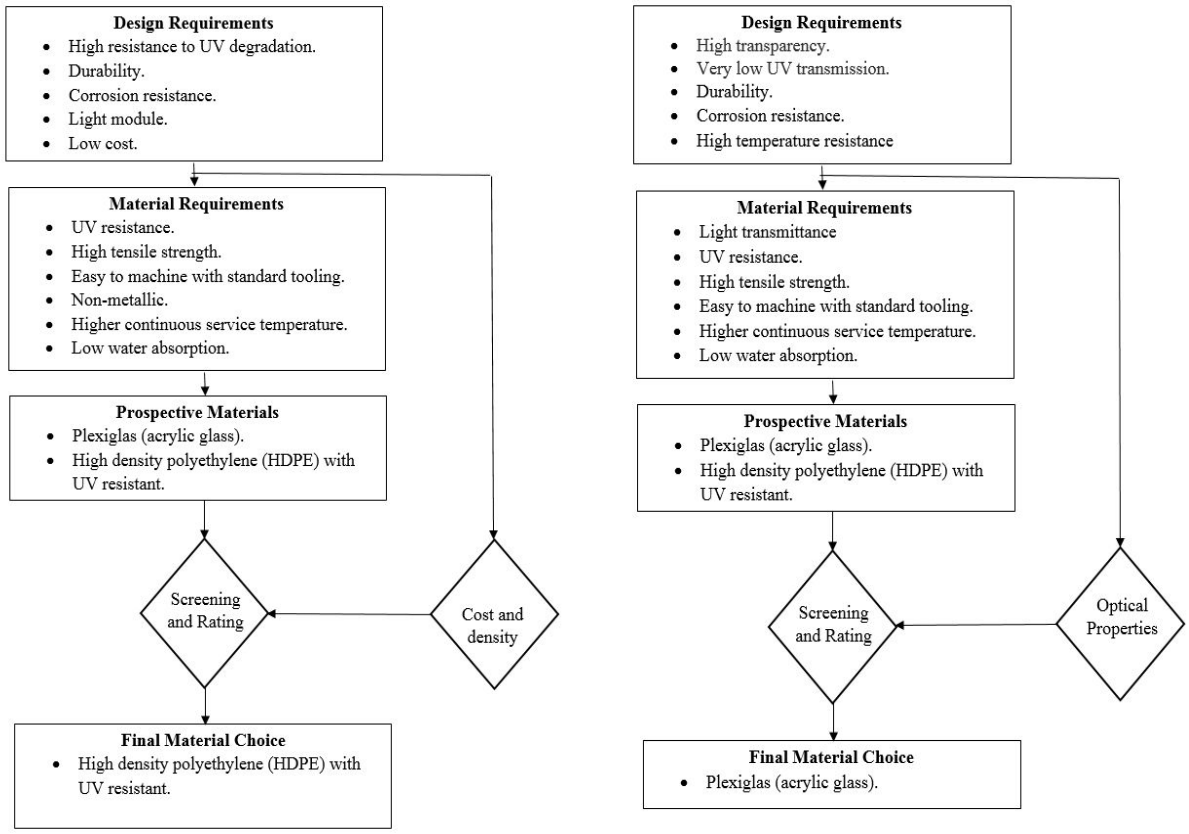

a. Disclosure plates b. Light transmittance window

Figure 6. Material selection diagrams

It is worth mentioning that the NESMD reactor is equipped with a Photovoltaic panel (0.70 x 0.52 x 0.025 m) at an inclination angle of 45^{o} to provide electric power for pumping the feed water and sweeping air to the reactor. Also, a solar charge controller is used in conjunction with the solar panel and two parallel-connected lead-acid batteries to avoid overcharging and control the power system. Figure 7 shows a schematic diagram for the electrical connections and power control.

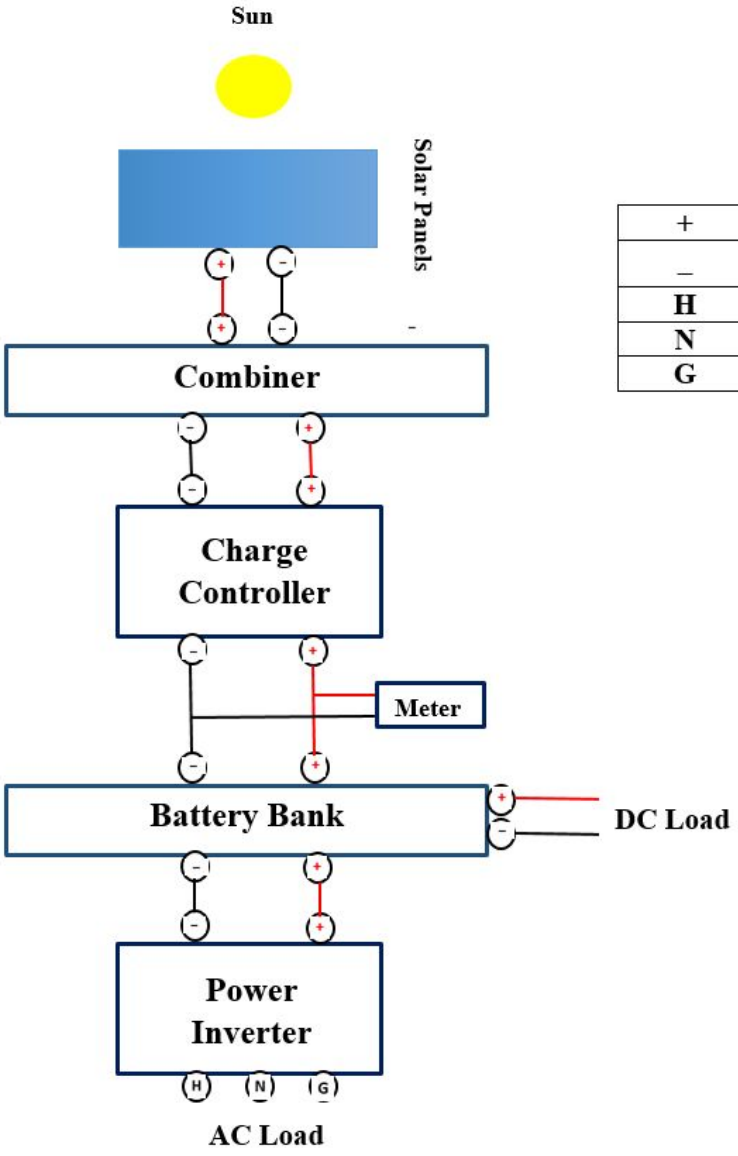

+	Positive Terminal
_	Negative Terminal
H	AC Hot
N	AC Neutral
G	AC Ground

Figure 7. Electrical connection system

The measurement system consists of a series of 1/16 T-thermocouples temperature sensors that were installed on the liquid and air-flow lines to the three-flow chambers to monitor and record the main process temperatures across the flow chambers. Three flow meters were installed to measure the volumetric flow rate of pretreated feed water to the third channel, the sweeping air to the middle channel, and preheated feed water to the top channel. Humidity meters were installed at the airlines to track the air relative humidity and an inline conductivity meter (Oakton pH/CON 510 series) was installed at the exit of the distillate channel to monitor the

salinity of the distillate. Furthermore, a digital solar meter (Solartech Inc. 00208) to measure the solar irradiation intensity has been used as well as a digital USB data logger for ambient humidity, ambient temperature, barometric pressure. The mass of the permeate over the time of the experiment has been monitored and recorded using a digital weighing balance. All system components, except the transmittance window of the photothermal membrane, were insulated to minimize the heat losses to the environment and consequently getting higher water flux. The quality of the permeate is monitored using a conductivity and TDS meters. It is worth mentioning that the NESMD reactor is attached to a mounting pole to control the angle and direction of the NESMD reactor (Figure 8). An angle of inclination of 35^{o} was chosen in all the experiments. The angle is corresponding to a light transmission of 92%. Approximately 8% of the incident rays are reflected at each air-surface interface of the colorless Plexiglas sheet[42].

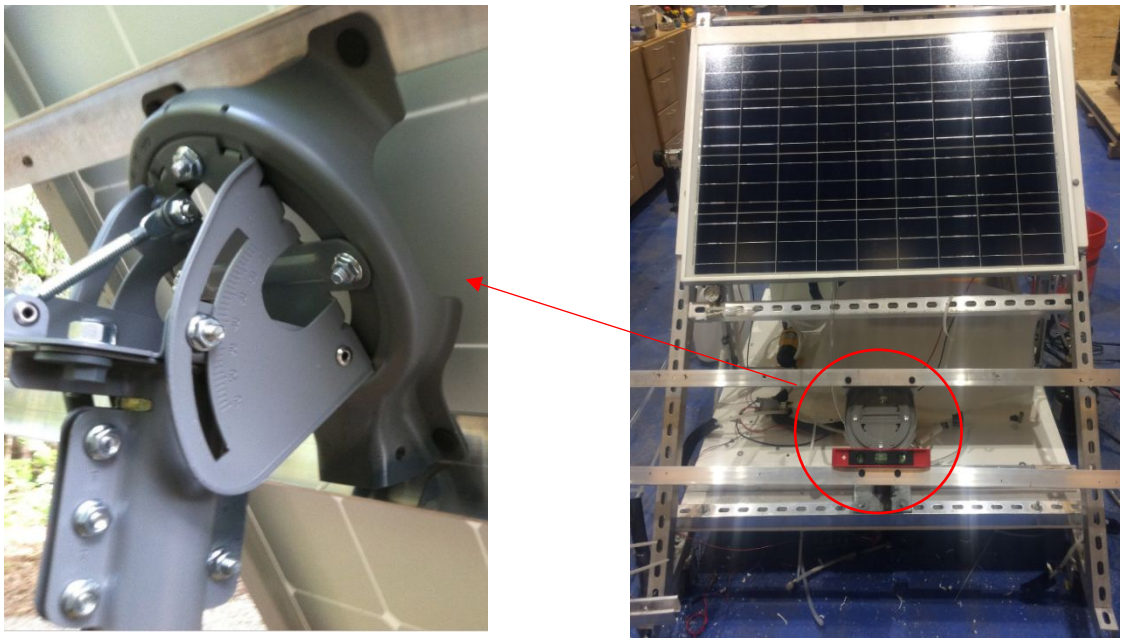

Figure 8. Mounting pole for the NESMD reactor

3.2 NESMD Prototype: System Operation

Pretreated cold feedwater enters the bottom channel and gains heat by internal heat recovery. The preheated feedwater then leaves the bottom channel and enters the solar top channel. The hot feed water flows through the top channel (evaporation) in co-current direction to the sweeping air in the middle channel. The exit hot feed water from the top channel is recirculated

back to the top channel. The generated water vapor passes through the photothermal membrane and condenses in the middle channel. The sensible heat and latent is transferred through the heat exchanger material foil (0.2 mm thickness) to preheat the feed water in the bottom channel. The sweeping air and condensed distillate exit the NESMD prototype at the permeate outlet to a product tank with a vent. It is worth mention that in all the experiments, there is no external condenser for heat recovery has been used. The NESMD system is self-running since the air pump, pumps, and control system are electrically powered by the photovoltaic panel. The operation of the NESMD prototype is only executed during day time because there is no other source of heat or electricity used. It is worth mentioning that in the absence of solar energy, the current system can be coupled with an external heater to serve as a conventional membrane distillation module.

4. Experimental conditions

SGMD experimental work has been executed using different sources of feed waters, simulated and real feedwaters, under different operating conditions, taking into consideration the environmental impacts. The real feed waters include low-salinity seawater from inner Galveston Bay, Galveston, Texas U.S. (TDS of ~20,000 PPM); high-salinity seawater from outer Galveston Bay, Galveston, Texas U.S. (TDS of ~40,000 PPM), while the simulated feed water tests include: TDS of 113,200, 121,700, 139,800, 172,600, and 200,000 PPM under different operating conditions, taking in consideration the environmental impacts. The environmental parameters include the speed of the air, barometric pressure, ambient temperature, relative humidity, and solar irradiance. In all these experiments, Polytetrafluoroethylene (PTFE) membrane on photothermal coated polypropylene (PP) support was used with 0.2 μm pore diameters, 25 μm photothermal coating thickness, and 77% porosity. It is worth mentioning that the simulated feedwaters (synthesized wastewater feed samples) were prepared by dissolving the analytical grade sodium chloride in deionized water.

Two different feed flow rates to the top channel have investigated, including 1.8 Liter/hour and 3.8 Liter/hour, while the airflow rate was ranging between 120-240 Liter/hour. In all the experiments, the flow rate of the bottom channel was set at 17 Liter/hour, which is much higher than the top channel to achieve a higher rate of heat transfer between the vapor in the middle channel and feed water in the bottom. The higher the feed flow rate, the higher the rate of heat transfer, and consequently better condensation for the vapor in the middle channel. It is worth mention that there is no external heat exchanger has been used in all experiments.

The experimental work starts by pumping the feed water from a five gallons feed tank into the bottom chamber of the NESMD module. The volumetric flow rate in the bottom channel was 17 Liter/hour. The outlet preheated feed flow is divided into two streams, one flows to the top channel, while the other one was continuously circulated in a counter-current flow mode with respect to the air in the middle channel, where feed in the bottom channel and distillate streams flow in the opposite directions (Figure 3). The reason behind splitting the exit feed flow from the bottom channel is that the feed flow rate in the top channel is much lower than the bottom channel.

The feed in the top channel was continuously circulated through the membrane module using a magnetic drive pump (NH-5PI-S-D Pan World Co., LTD.) in a co-current flow mode, where the feed water in the top channel and distillate streams flow in the same directions (Figure 3). The main purpose of the top feed recirculation loop is to enhance the performance of the NESMD reactor in terms of maximizing the heat recovery and thermal efficiency. This recirculation step allows the use of the sensible heat lost within in the form of the heated feed output of NESMD and consequently increase the overall permeate production of the NESMD system by reducing the brine production from the NESMD reactor. The solar rays penetrating through the Plexiglas transmittance window raise the temperature of the photothermal membrane. It transfers the heat of the sun to the feedwater to get evaporated.

A series of 1/16 T-thermocouples temperature sensors were installed on the liquid and air-flow lines to the three-flow chambers to monitor and record the main process temperatures across the flow chambers. Three flow meters were installed to measure the volumetric flow rate of pretreated feed water to the third channel, the sweeping air to the middle channel, and preheated feed water to the top channel. Furthermore, a digital solar meter (Solartech Inc. 00208) to measure the solar irradiation intensity has been used as well as a digital USB data logger for humidity, ambient temperature, barometric pressure. The mass of the permeate over the time of the experiment has been monitored and recorded using a digital weighing balance. All system components, except the transmittance window of the photothermal membrane, were insulated to minimize the heat losses to the environment and consequently getting higher water flux. All the processes and environmental parameters were recorded every 15 minutes. The measured data in this work has measured and collected in summer 2019 at 29.7174° N, 95.4018° W.

Results and discussion

The performance of the NESMD system using real and simulated feed waters is shown in Figures 9-22 for selected experiments. The system started operation at ~10:30 am when the solar irradiation was in the range of ~300 W/m^2. The process temperature fields across the three-flow chambers are presented for different ranges of TDS and operating conditions as shown in Figures 9-13 for selected experiments. It is clear from all the figures (9-13) that the bottom chamber is getting more energy from the vapor in the middle channel (condensation), which is clear in the temperature gained across the bottom chamber ($T_{in,bottom}$ and $T_{out,bottom}$). Furthermore, a small temperature difference is noticed across the top channel. This could be attributed to that the heat absorbed by the photothermal membrane was used to evaporate the adjacent layer of the liquid at the membrane interface. Figures 14-17 show the variation of the relative humidities of the sweeping air across the middle channel. A small difference in the values of the relative humidity of the air (in and out) is observed and sometimes, the relative humidity or the air out is a little bit lower than the air inlet. This confirms that the majority of generated vapor is condensed within the middle channel.

The permeate production rate was normalized using the effective membrane surface area (0.2 m^2) and illustrated in Figures 18-21 for selected experiments as a function of the solar irradiation (permeate flux expressed as kg/m^{2}hr). The local permeate flux reached above 0.75 kg/m^2 hr when the solar irradiation was about 1000 W/m^2 with >99.5% TDS removal for all experimental conditions. It is clear from the permeate figures that the permeate flux increased with the increase of solar irradiation and decreased with the increase in the feed salinity. In all the experimental runs, the environmental parameters, including the speed of the ambient air, ambient relative humidity, ambient temperature, barometric pressure, solar irradiation have monitored and will be used in another work for quantifying the heat losses from the NESMD reactor (Figure 22). In all the Figures (18-22) of solar irradiance, one can remark fluctuations in the measured values of solar radiation. The amount of solar radiation reaching the NEMSD 's membrane surface changes greatly because of the changing position of the sun and varying atmospheric conditions, both during the day. Clouds are the predominant atmospheric condition that decides the intensity of solar radiation that reaches the NESMD membrane. Hence, the fluctuations in the values of the solar irradiance could be attributed to the clouds, which turns the solar irradiance down.

Tables 1-2 summarizes all the experiments for different operating conditions. Tables 1-2 show the water qualities of the feed waters and permeate in terms of TDS and conductivity, it is clear that TDS and conductivity removals are greater than >95% and meeting the World Health Organization (WHO) standards.

It is worth mentioning that the current NESMD reactor is still in an early stage of Research and Development (R&D). Further investigations, improvements, optimization are required to enhance the performance of the NESMD reactor. Focusing the sunlight over the NEMD membrane is considering one of the potential solutions for improving the production of purified water from the NESMD system. Concentrating the sunlight on the photothermal membrane leads in a linear gain in the amount of heat, and consequently generates a nonlinear increase in the water vapor pressure. Hence, the produced clean water is exponentially dependent on the solar intensity[43].

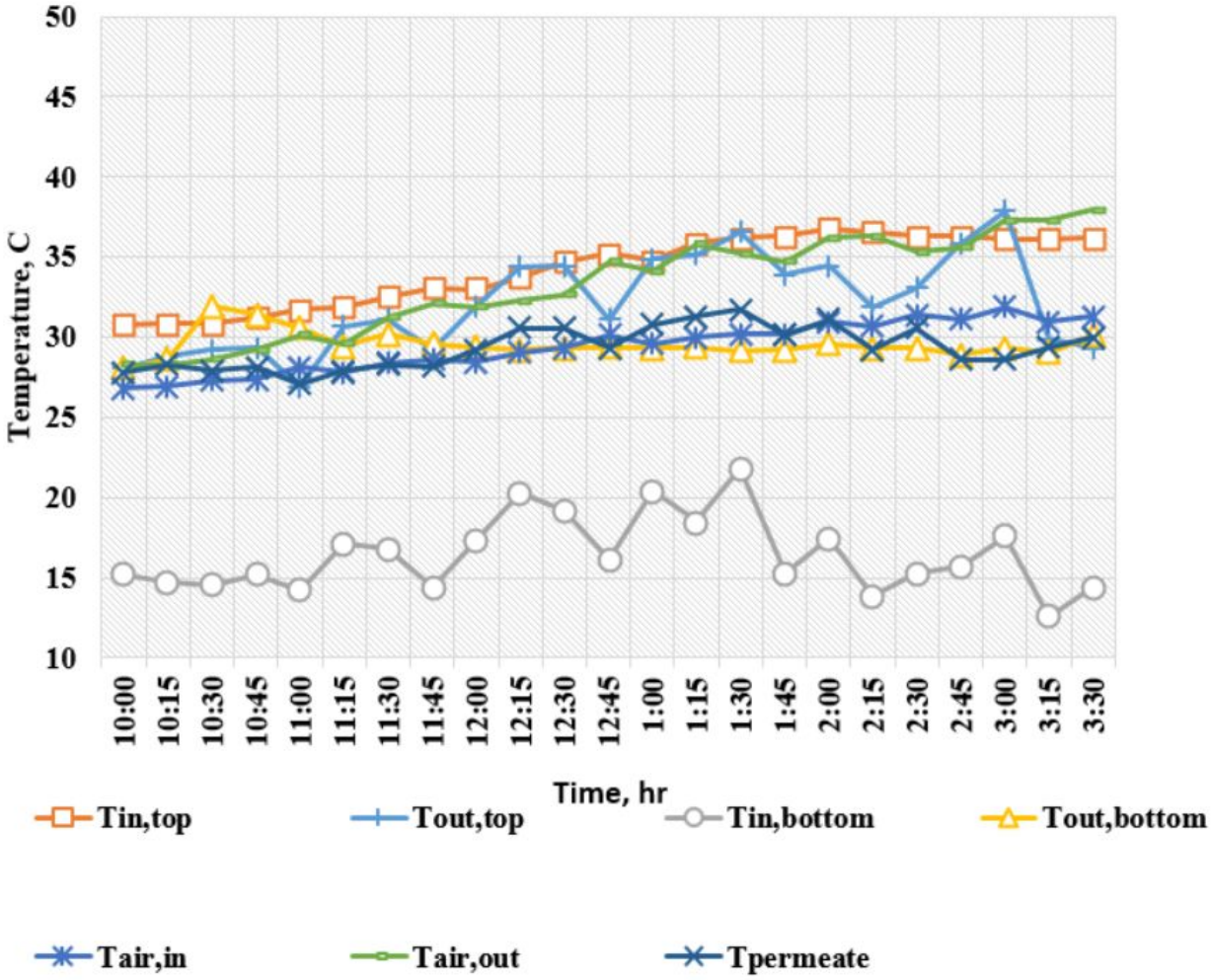

Figure 9. Field temperature distributions across the three flow chambers as a function of the solar irradiation and relative humidity (High salinity Galveston seawater, TDS of 40,040 ppm with a TDS removal of 99.6% - flow rates of the top channel 1.8 Liter/hour, bottom channel 17 Liter/hour, and air 120 Liter/hour)

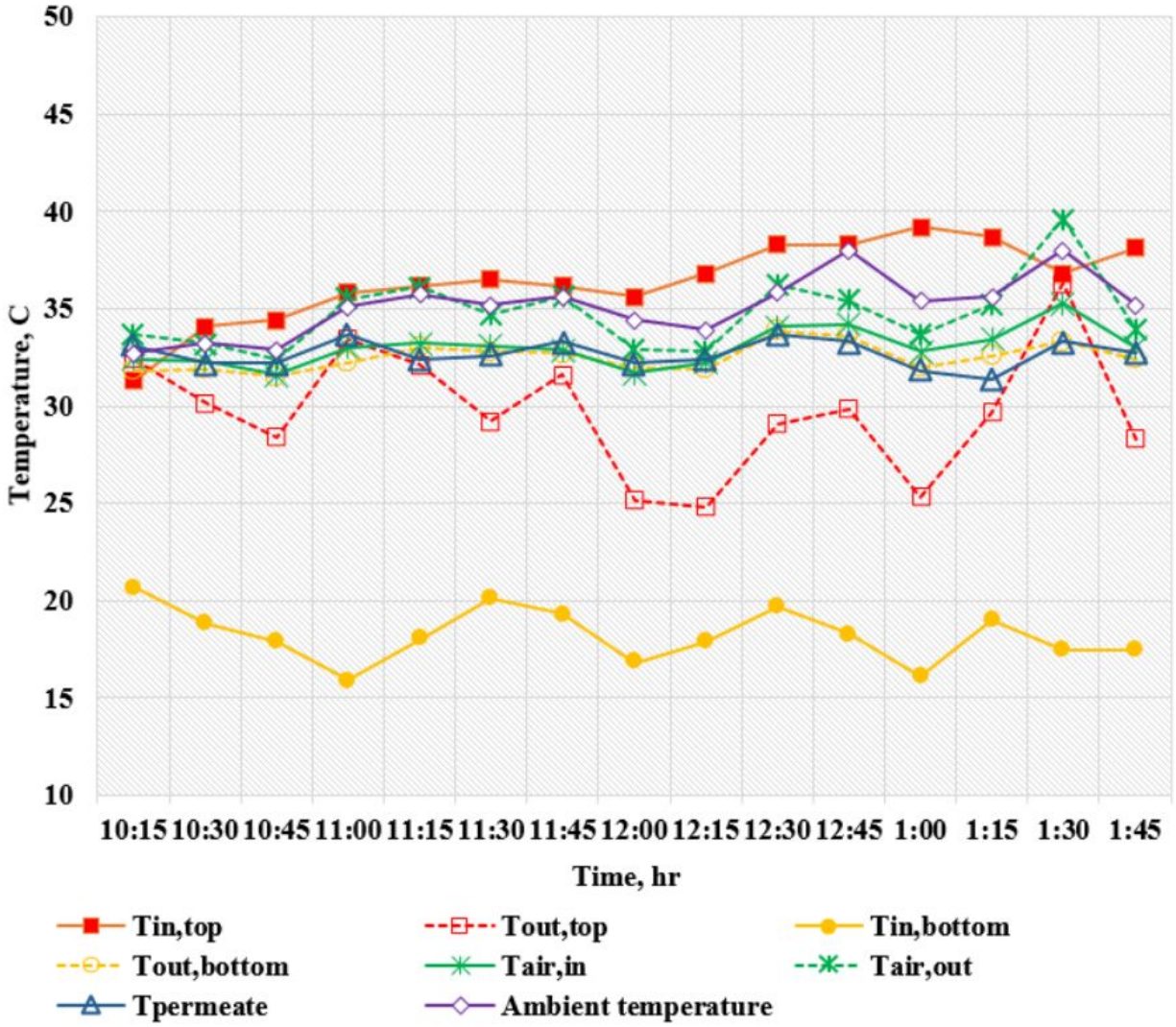

Figure 10. Field temperature distributions across the three flow chambers (simulated feed water, TDS of 113,200 ppm with a TDS removal of 99.6% - flow rates of top channel 1.8 Liter/hour, bottom channel 17 Liter/hour, and air 120 Liter/hour)

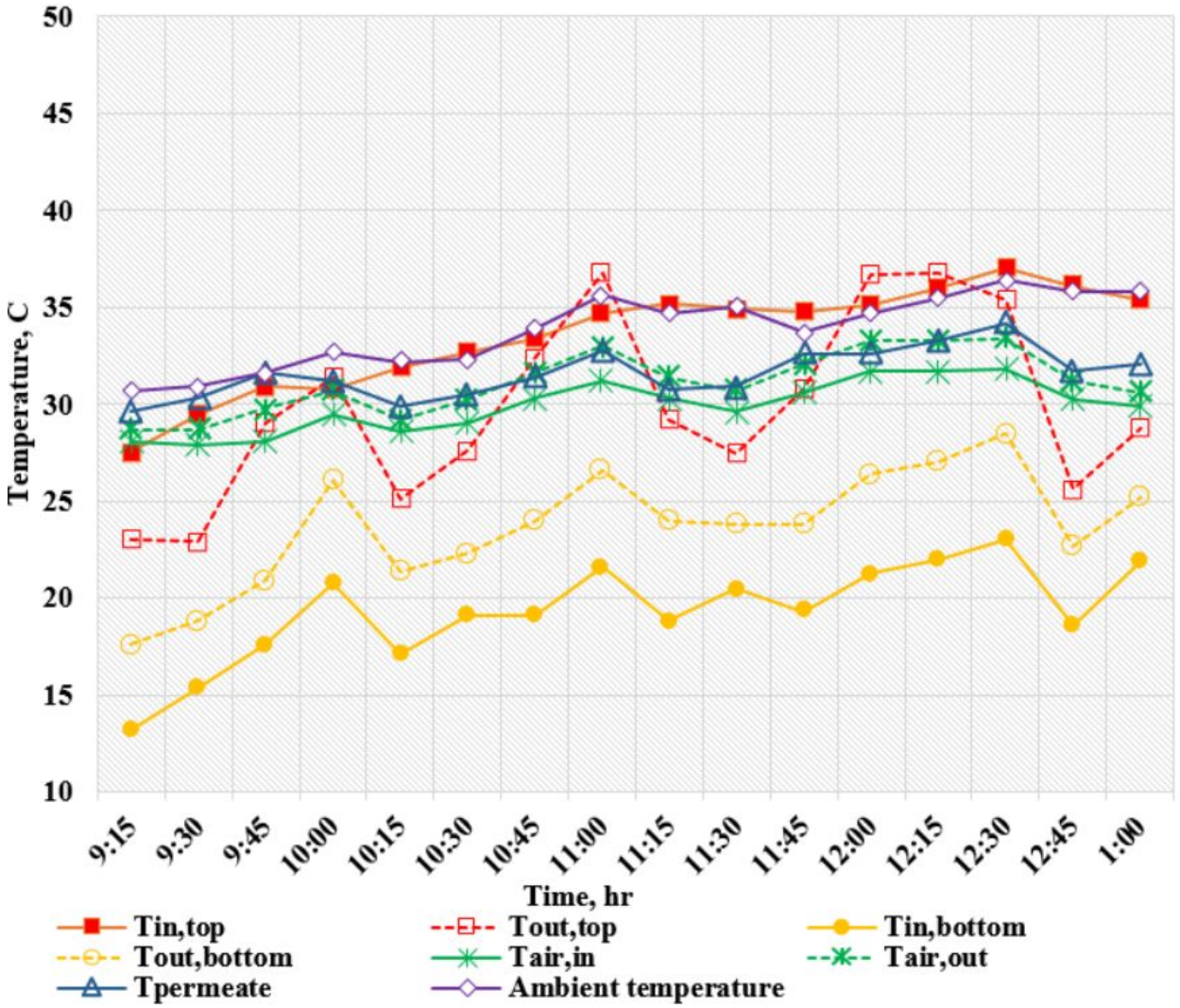

Figure 11. Field temperature distributions across the three flow chambers (simulated feed water, TDS of 121,700 ppm with a TDS removal of 99.5% - flow rates of the top channel 1.8 Liter/hour, bottom channel 17 Liter/hour, and air 120 Liter/hour)

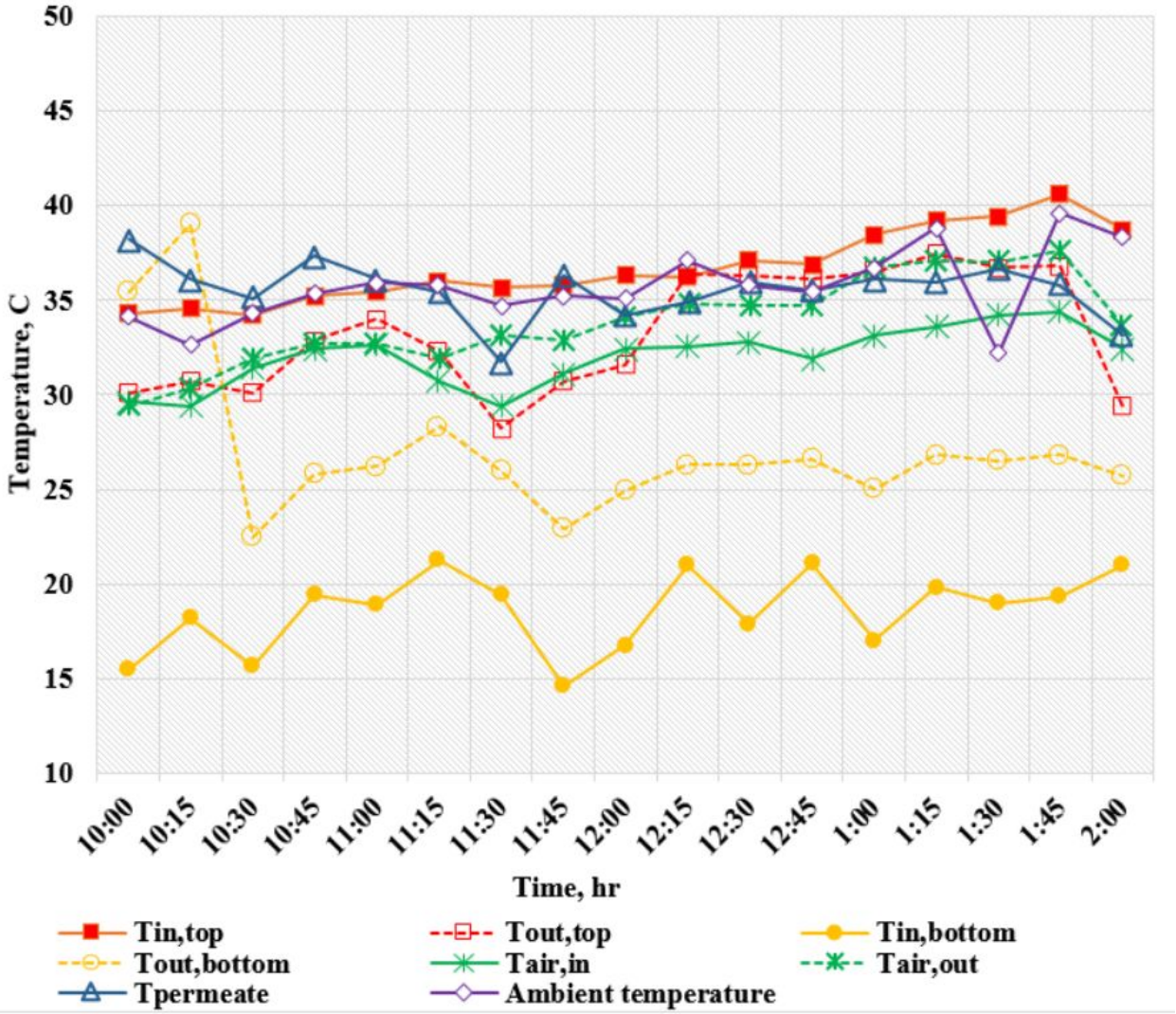

Figure 12. Field temperature distributions across the three flow chambers (simulated feed water, TDS of 172,600 ppm with a TDS removal of 99.5% - flow rates of the top channel 1.8 Liter/hour, bottom channel 17 Liter/hour, and air 120 Liter/hour)

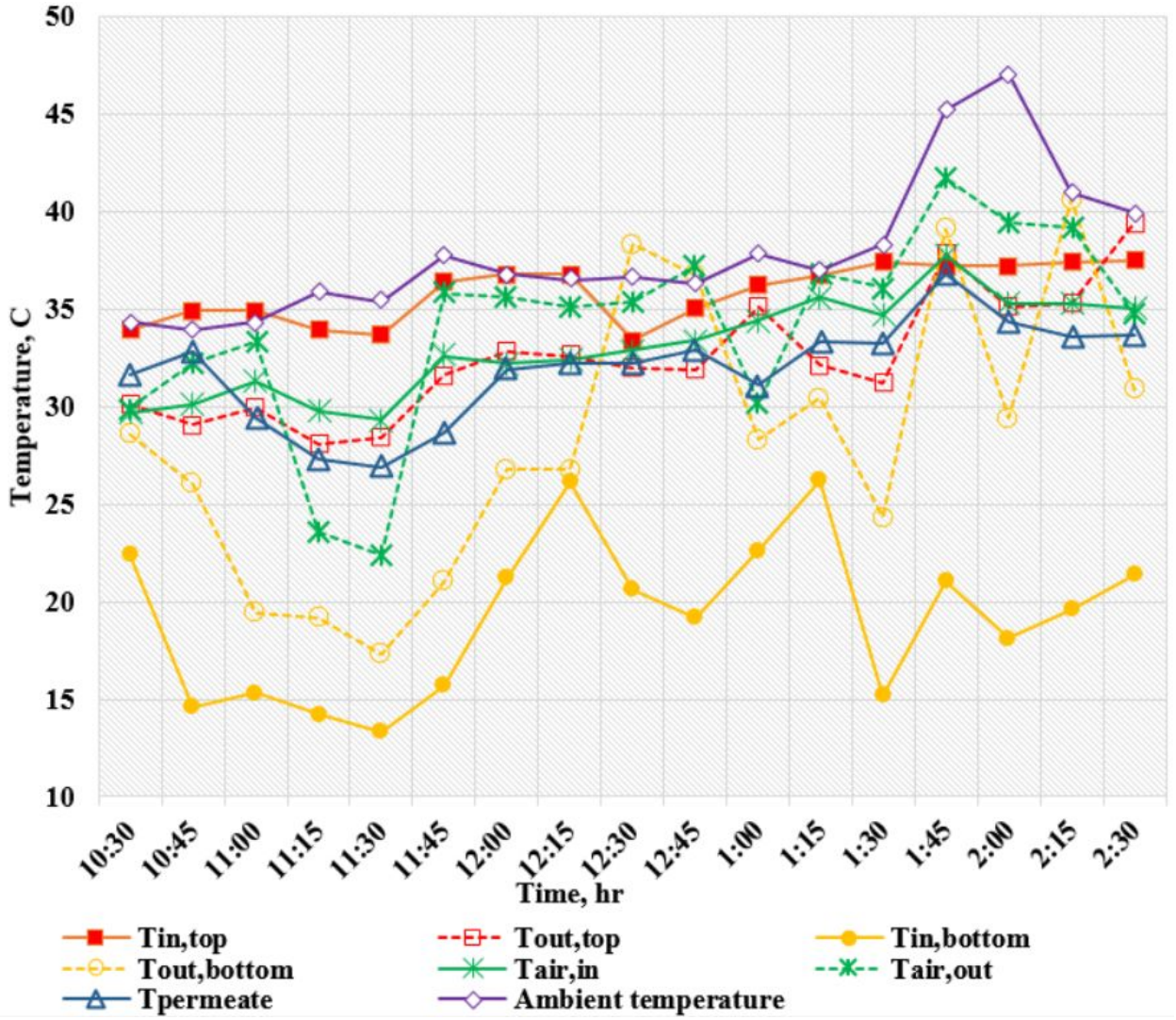

Figure 13. Field temperature distributions across the three flow chambers (simulated feed water, TDS of 139,800 ppm with a TDS removal of 99.5% - flow rates of the top channel 1.8 Liter/hour, bottom channel 17 Liter/hour, and air 120 Liter/hour)

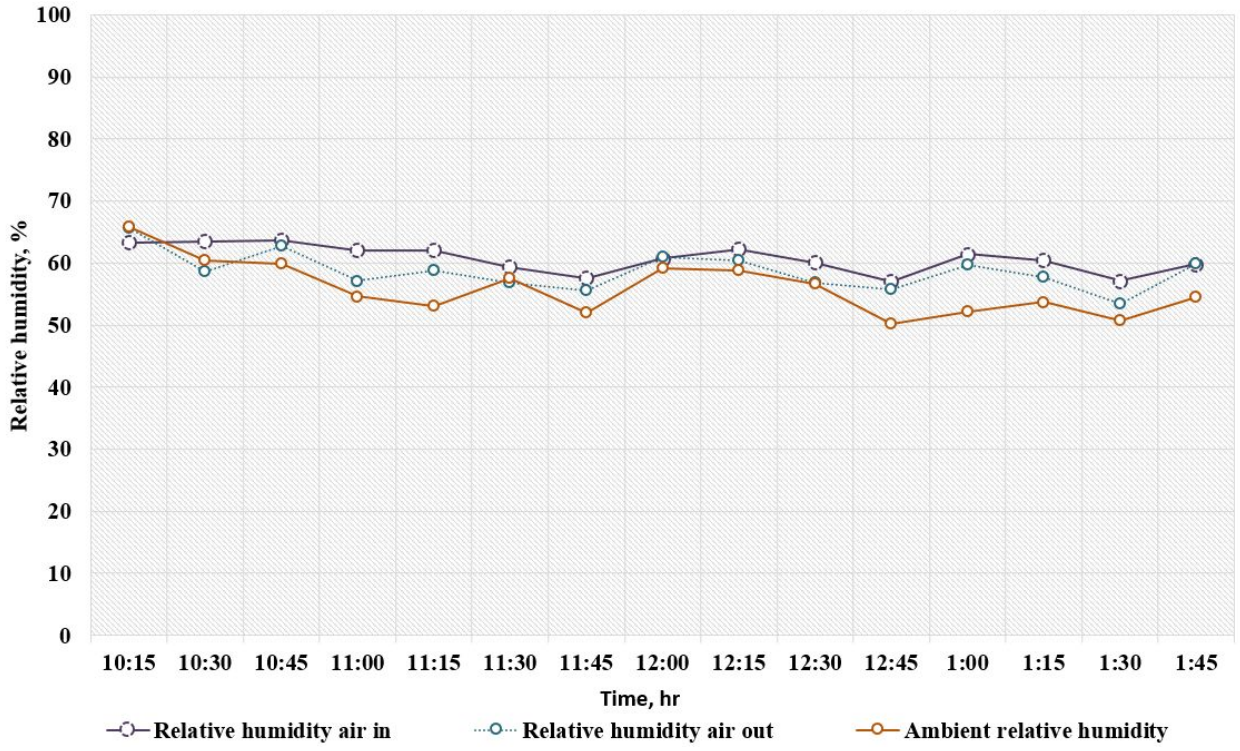

Figure 14. Relative humidity across the air channel as a function of solar irradiance (simulated feed water, TDS of 113,200 ppm with a TDS removal of 99.6% - flow rates of top channel 1.8 Liter/hour, bottom channel 17 Liter/hour, and air 120 Liter/hour)

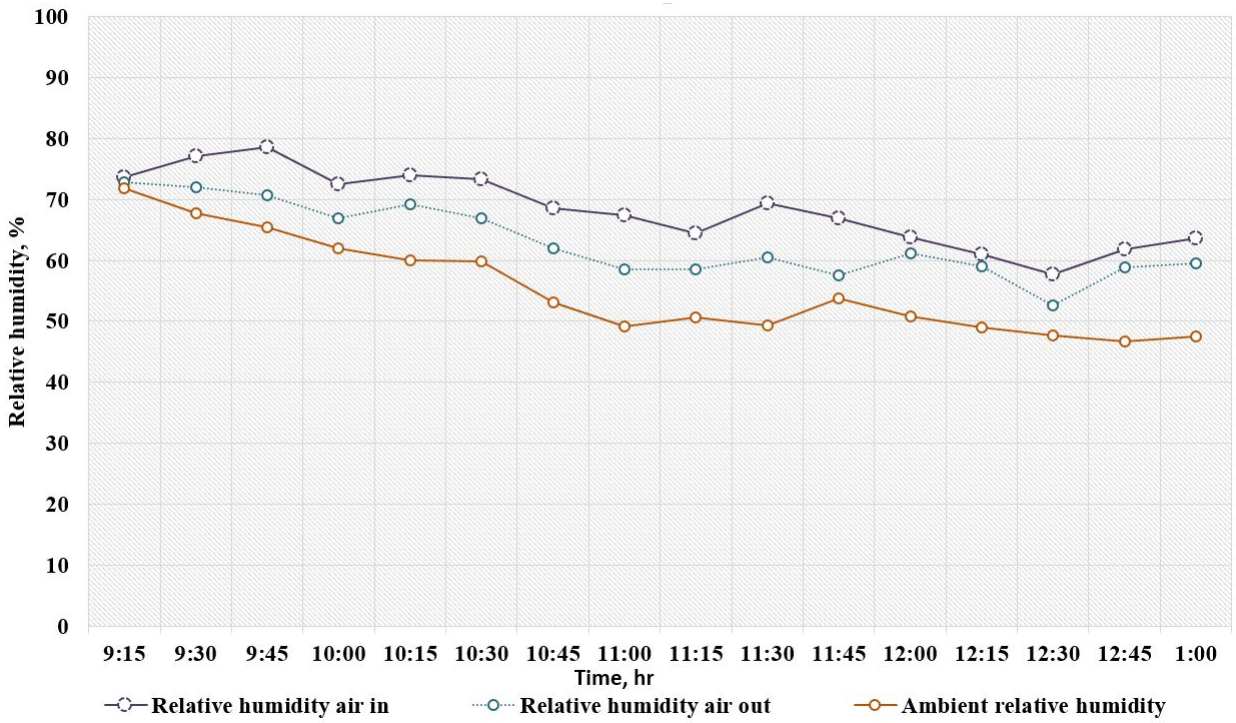

Figure 15. Relative humidity across the air channel as a function of solar irradiance (simulated feed water, TDS of 121,700 ppm with a TDS removal of 99.5% - flow rates of the top channel 1.8 Liter/hour, bottom channel 17 Liter/hour, and air 120 Liter/hour)

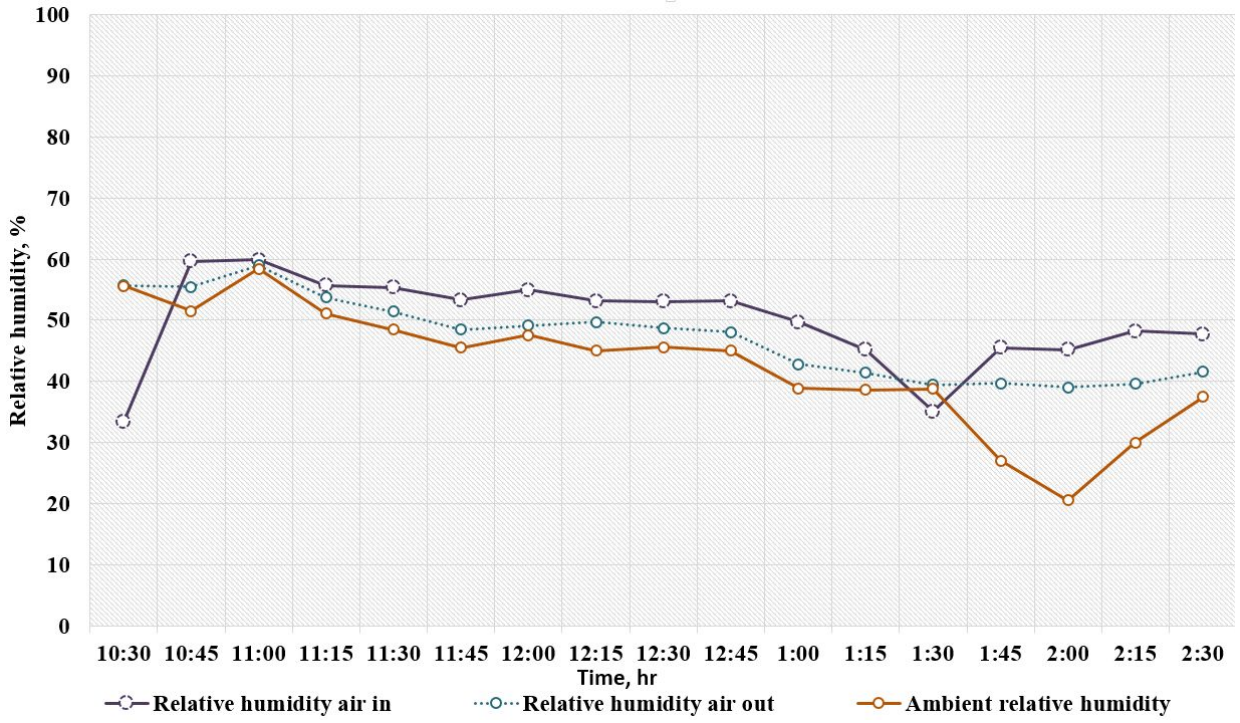

Figure 16. Relative humidity across the air channel as a function of solar irradiance (simulated feed water, TDS of 139,800 ppm with a TDS removal of 99.5% - flow rates of the top channel 1.8 Liter/hour, bottom channel 17 Liter/hour, and air 120 Liter/hour)

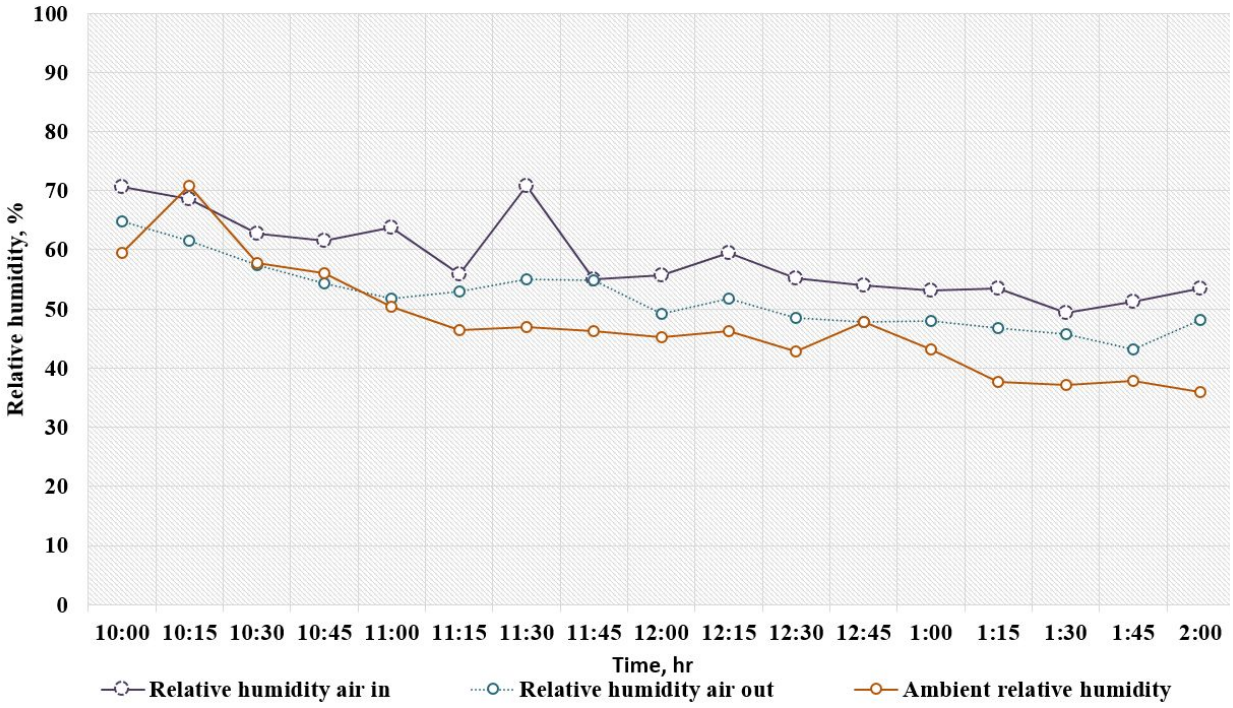

Figure 17. Relative humidity across the air channel as a function of solar irradiance (simulated feed water, TDS of 172,600 ppm with a TDS removal of 99.5% - flow rates of the top channel 1.8 Liter/hour, bottom channel 17 Liter/hour, and air 120 Liter/hour)

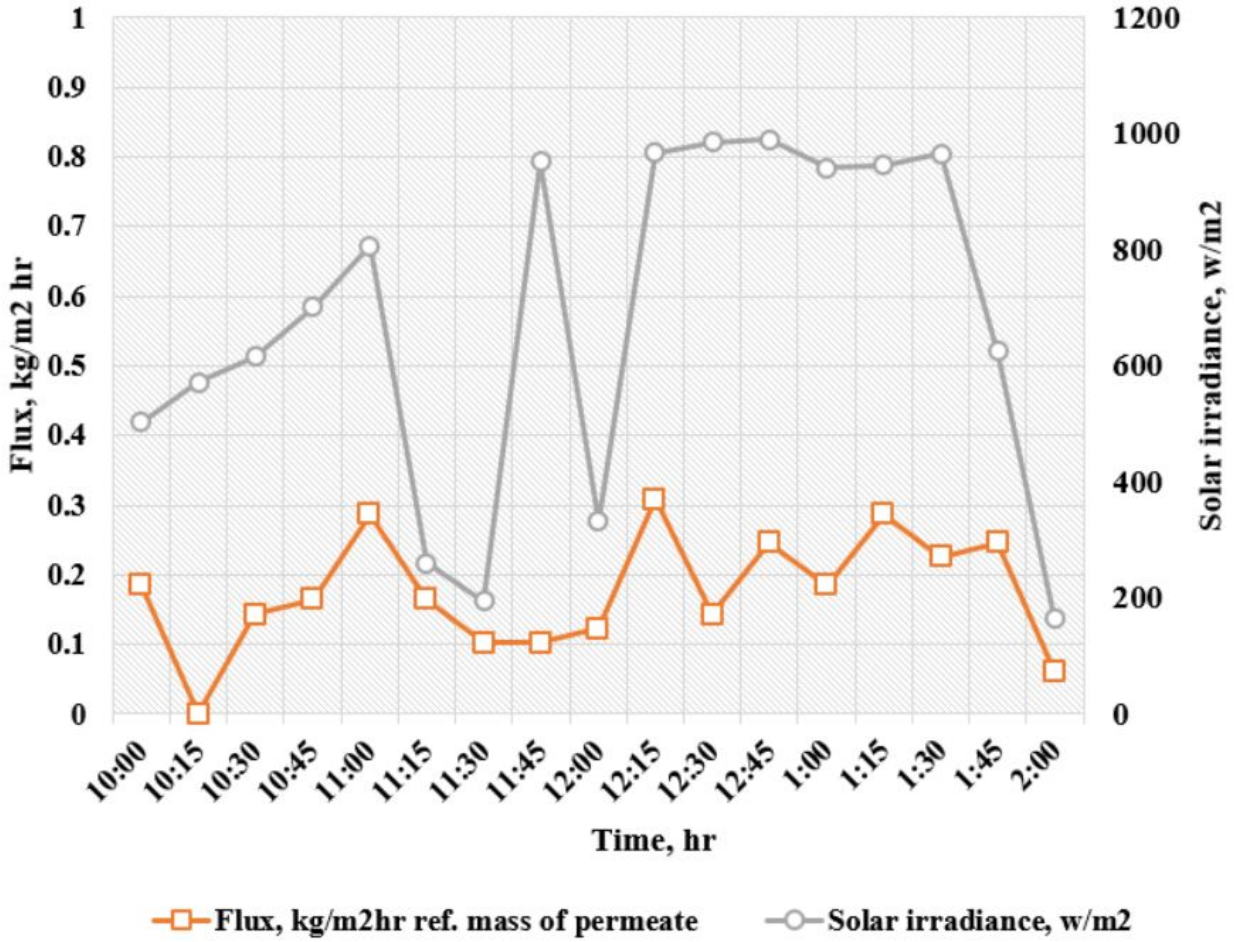

Figure 18. Time series of the permeate flux as a function of the solar irradiation (simulated feed water, TDS of 172,600 ppm with a TDS removal of 99.5% - flow rates of the top channel 1.8 Liter/hour, bottom channel 17 Liter/hour, and air 120 Liter/hour)

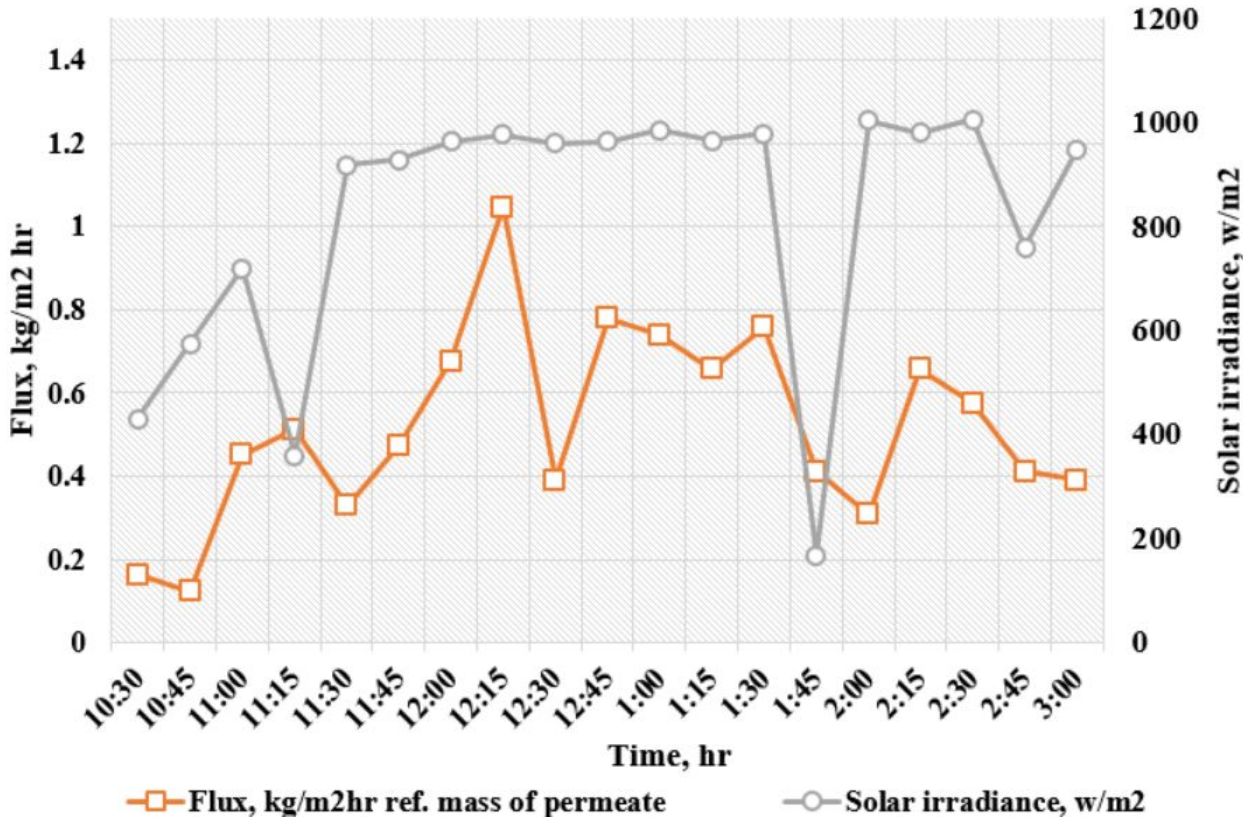

Figure 19. Time series of the permeate flux as a function of the solar irradiation (Low salinity Galveston seawater, TDS of 21,340ppm with a TDS removal of 99.4% - flow rates of top channel 1.8Liter/hour, bottom channel 17 Liter/hour, and air 120 Liter/hour).

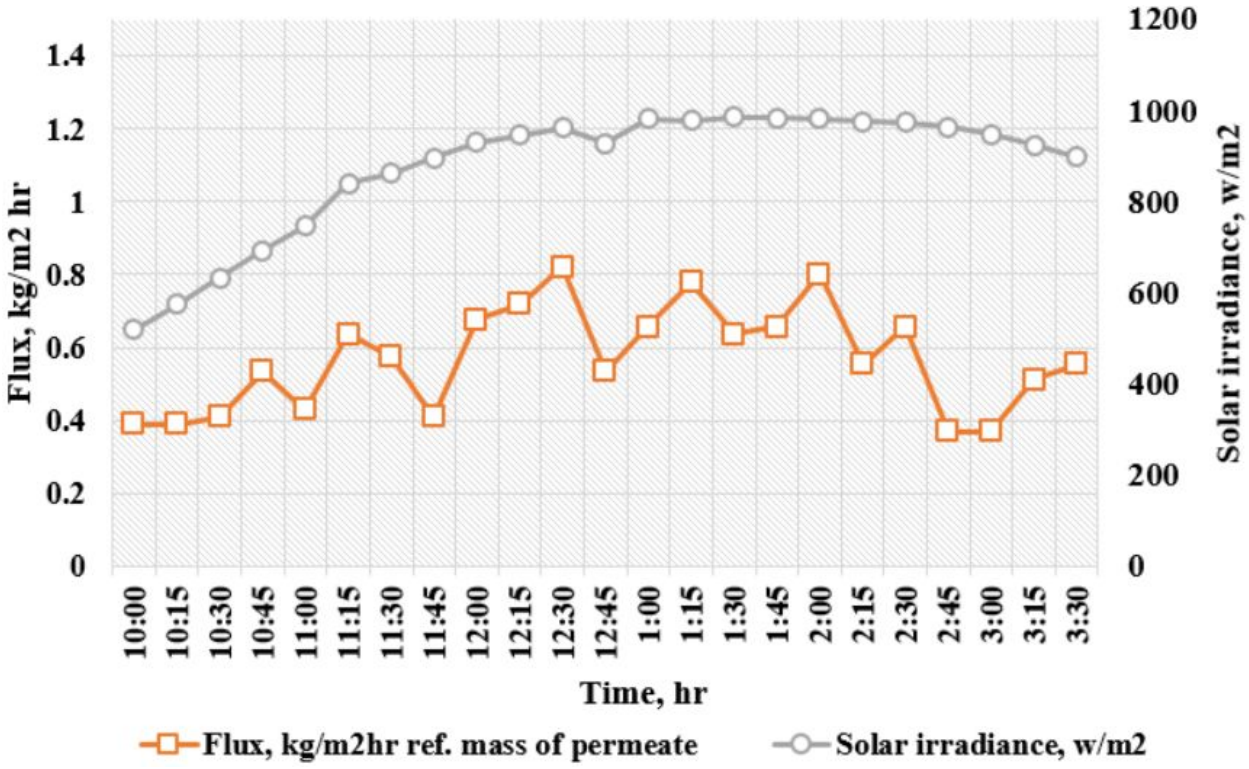

Figure 20. Time series of the permeate flux as a function of the solar irradiation (High salinity Galveston seawater, TDS of 40,040 ppm with a TDS removal of 99.6% - flow rates of the top channel 1.8 Liter/hour, bottom channel 17 Liter/hour, and air 120 Liter/hour).

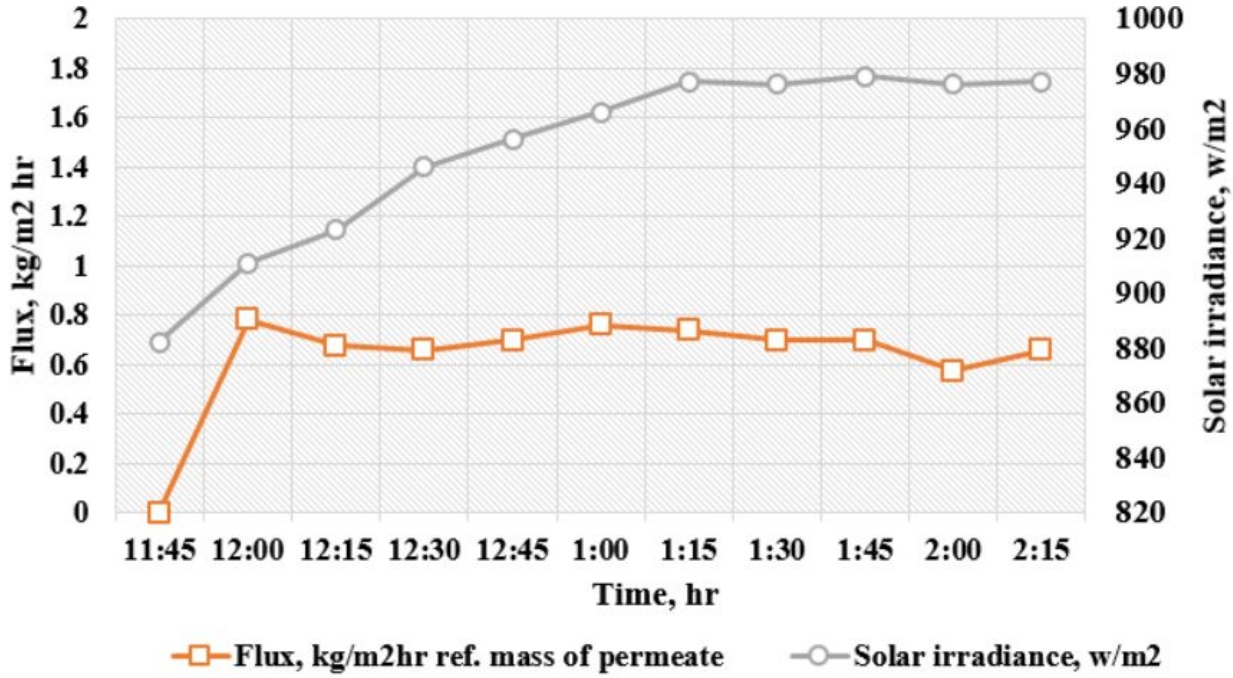

Figure 21. Time series of the permeate flux as a function of the solar irradiation (High salinity Galveston seawater, TDS of 40,090 ppm with a TDS removal of 99.7% - flow rates of the top channel 3.8 Liter/hour, bottom channel 17 Liter/hour, and air 120 Liter/hour).

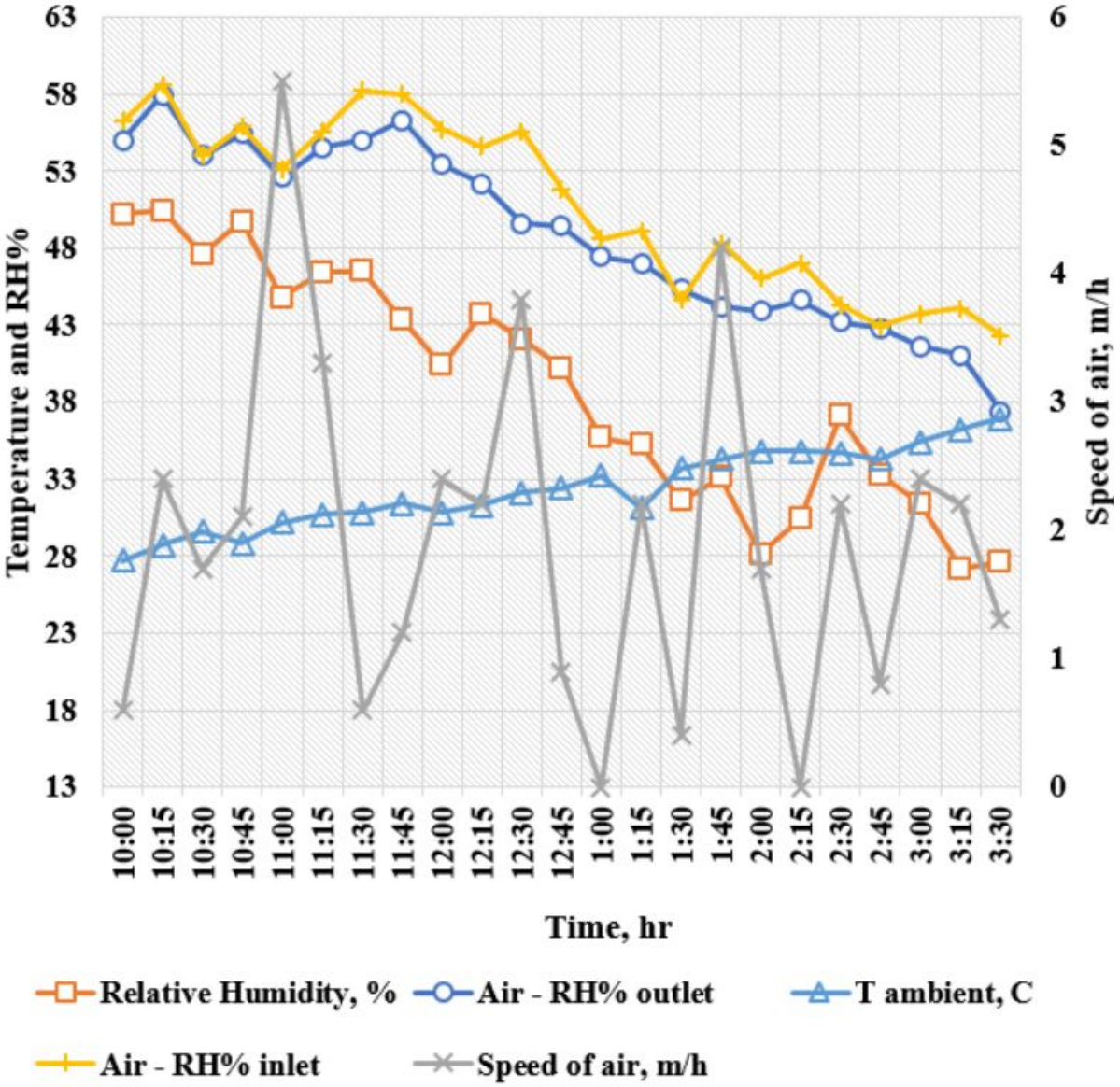

Figure 22. Selected environmental parameters on July 24, 2019, for testing high salinity Galveston seawater, TDS of 40,040 ppm with a TDS removal of 99.6% - flow rates of the top channel 1.8 Liter/hour, bottom channel 17 Liter/hour, and air 120 Liter/hour.

Table 1. A summary of the outdoor lab-scale NESMD experiments (flow rate of the top channel: 1.8 Liter/hour, middle channel: 120 L/hour, and the bottom channel: 17 Liter/hour).

Feedwater	**TDS Feed, ppm**	**Average Flux, kg/m^{2}hr**	**Average solar irradiance, w/m^2**	**TDS removal, %**
Low salinity Galveston Seawater	21,340	0.547±0.229	819±253	99.5
High salinity Galveston Seawater	40,040	0.547±0.142	819±141	99.6
Simulated feed water	113,200	0.263±0.124	460±372	99.5
	121,700	0.135±0.088	389±280	99.6
	139,800	0.289±0.107	828±212	99.8
	172,600	0.185±0.085	677±299	99.5
	200,000	0.120±0.098	600±141	99.9

Table 2. A summary of the outdoor lab-scale NESMD experiments (flow rate of the top channel: 3.8 Liter/hour, middle channel: 120-240 Liter/hour, and bottom channel: 17 Liter/hour).

Feedwater	TDS Feed, ppm	Average Flux, kg/m^{2}hr	Solar irradiance, w/m^2	TDS removal, %
High salinity Galveston Seawater (120L/hour air)	40,090	0.7548±0.216	951.72± 33	99.7
Simulated feed water (240 L/hour air)	101,400	0.175±0.139	542.23±292	99.5

Remarks

A novel stand-alone Nanophotonics Enabled Solar Membrane distillation (NESMD) technology is developed and tested for desalinating real seawater from Galveston Bay, Texas U.S. and high salinity simulated feed waters (TDS of 113,200, 121,700, 139,800, 172,600, and 200,000 PPM). The NESMD reactor is consisting of three-flow channels for evaporation, condensation, and heat exchange. Whenever sufficient solar irradiance is present to heat up the photothermal membrane and electricity for pumping the feedwater and air to produce distillate water. The experiments executed out so far at Houston, Texas U.S. weather conditions showed very promising results. The TDS removal was ≥ 99.5% in all experiments. Average daily membrane flux of ≥ 0.75 L/m^2-hr was achieved at a solar intensity close to 1 kW/m^2 without external heat exchange. It is worth mentioning that the NESMD technology is raising a commercial growing interest due to its special advantages, including 1) No need for external heaters and solar collection system, 2) operating at low-feed temperature, 3) high quality of permeate water, 4) potential solution for high salinity water and Zero-liquid discharge, and 4) off-grid operation.

Acknowledgment

This work was funded by the U.S. Department of Energy – Solar Energy Technologies Office (Award # DE-EE0008397) and NSF NERC on Nanotechnology-Enabled Water Treatment (NEWT-EEC 1449500).

References

1. Bruggen, B. Van der and C. Vandecasteele, *Distillation vs. membrane filtration: overview of process evolutions in seawater desalination.* Desalination, 2002. **143**(3): p. 207-218.
2. Kim, Y.M., S.J. Kim, Y.S. Kim, S. Lee, I.S. Kim, and J.H. Kim, *Overview of systems engineering approaches for large scale seawater desalination plant with reverse osmosis network.* Desalination, 2009. **238**: p. 312-332.
3. Association, International Desalination, *International Desalination Association and Global Water Intelligence Release New Data in 30th Worldwide Desalting Inventory.* 2017.
4. Elimelech, M. and W. A. Phillip, *The future of seawater desalination: energy, technology, and the environment.* Science, 2011. **333**(6043): p. 712-717.
5. Service, Robert F., *Desalination Freshens Up.* Science, 2006. **313**(5790): p. 1088-1090.
6. Veil, John A., et al. , *A white paper describing produced water from production of crude oil, natural gas, and coal bed methane.* No. ANL/EA/RP-112631. Argonne National Lab., IL (US), 2004.
7. Clark, C. E. and J. A. Veil, *Produced water volumes and management practices in the United States.* Argonne National Lab.(ANL), Argonne, IL (United States), 2009.
8. Fakhru'l-Razi, Ahmadun, and et al., *Review of technologies for oil and gas produced water treatment.* Journal of hazardous materials 2009. **170**(2-3): p. 530-551.
9. Igunnu, Ebenezer T. and George Z. Chen, *Produced water treatment technologies.* International Journal of Low-Carbon Technologies 2012. **9**(9): p. 157-177.
10. IEA. *World Energy Outlook*. 2018; Available from: https://www.iea.org/reports/world-energy-outlook-2018.
11. EIA, *Short-Term Energy Outlook (STEO)*. 2019.
12. Troner, AL, *Shale Gas and Tight Oil.* The James A. Baker III Institute For Public Policy Of Rice University, 2014: p. 1-139.
13. Hughes, J. David., *Energy: A reality check on the shale revolution.* Nature Energy, 2013. **494**: p. 307–308.
14. Kondash, Andrew J., Elizabeth Albright, and Avner Vengosh, *Quantity of flowback and produced waters from unconventional oil and gas exploration.* Science of the Total Environment, 2017. **574**: p. 314-321.
15. Khayet, Mohamed and Takeshi Matsuura, *Membrane Distillation Principles and Applications*. 2011: Elsevier.
16. Lawson, K. W. and D.R. Lloyd, *Membrane distillation.* Journal of Membrane Science, 1997. **124**(1): p. 1-25.
17. Alklaibi, A. M. and Noam Lior, *Membrane-distillation desalination: Status and potential.* Desalination, 2005. **171**(2): p. 111-131.
18. Smolders, K. and A.C.M. Franken, *Terminology for Membrane Distillation* Desalination, 989. **72**: p. 249-262.
19. Boi, C., S. Bandini, and G.C. SARTI', *Pollutants removal from wastewater through membrane distillation.* Desalination, 2005. **183**: p. 383-394.
20. G.C.Sarti, C.Gostoli, and S.Bandini, *Extraction of organic components from aqueous streams by vacuum membrane distillation.* Journal of Membrane Science, 1993. **80**(1): p. 21-33.
21. Banat, Fawzi A. and Jana Simandl, *Removal of benzene traces from contaminated water by vacuum membrane distillation.* Chemical Engineering Science, 1996. **51**(8): p. 1257-1265.
22. Kujawa, Joanna, Sophie Cerneaux, and Wojciech Kujawski, *Removal of hazardous volatile organic compounds from water by vacuum pervaporation with hydrophobic ceramic membranes.* Journal of Membrane Science, 2015. **474**: p. 11-19.

23. N.Couffin, C.Cabassud, and V. Lahoussine-Turcaud, *A new process to remove halogenated VOCs for drinking water production: vacuum membrane distillation.* Desalination, 1998. **117**(1–3): p. 233-245.
24. Duyen, Pham Minh, Paul Jacob, Romchat Rattanaoudom, and Chettiyapan Visvanathan, *Feasibility of sweeping gas membrane distillation on concentrating triethylene glycol from waste streams.* Chemical Engineering and Processing: Process Intensification, 2016. **110**: p. 225-234.
25. Shirazia, Mohammad Mahdi A., Ali Kargaria, Meisam Tabatabaeid, Ahmad Fauzi Ismailc, and Takeshi Matsuurac, *Concentration of glycerol from dilute glycerol wastewater usingsweeping gas membrane distillation.* Chemical Engineering and Processing, 2014. **78**: p. 58–66.
26. Bagger-Jørgensen, Rico, Anne S. Meyer, Manuel Pinelo, Camilla Varming, and Gunnar Jonsson, *Recovery of volatile fruit juice aroma compounds by membrane technology: Sweeping gas versus vacuum membrane distillation.* Innovative Food Science & Emerging Technologies, 2011. **12**(3): p. 388-397.
27. Rivier, C.A., M.C. Garc´ıa-Payo, I.W. Marison, and U. von Stockar, *Separation of binary mixtures by thermostatic sweeping gas membrane distillation I. Theory and simulations.* Journal of Membrane Science 2002. **201**: p. 1–16.
28. Calabro, Vincenza, Bi Lin Jiao, and Enrico Drioli, *Theoretical and Experimental Study on Membrane Distillation in the Concentration of Orange Juice.* Ind. Eng. Chem. Res., 1994. **33**(7): p. 1803-1808.
29. G.Zakrzewska-Trznadel, M.Harasimowicz, and A.G.Chmielewski, *Concentration of radioactive components in liquid low-level radioactive waste by membrane distillation.* Journal of Membrane Science, 1999. **163**(2): p. 257-264.
30. M.Tomaszewska, M.Gryta, and A.W.Morawski, *Study on the concentration of acids by membrane distillation.* Journal of Membrane Science, 1995. **102**: p. 113-122.
31. Francis, Lijo, Noreddine Ghaffour, Ahmad S. Alsaadi, Suzana P. Nunes, and Gary L. Amy, *PVDF hollow fiber and nanofiber membranes for fresh water reclamation using membrane distillation.* Journal of Materials Science, 2014. **49**(5): p. 2045–2053.
32. Curcioab, Xiaosheng Jia Efrem, Sulaiman Al Obaidanic, Gianluca Di Profioab, Enrica Fontananovaab, and Enrico Drioliab, *Membrane distillation-crystallization of seawater reverse osmosis brines.* Separation and Purification Technology, 2010. **71**(1): p. 76-82.
33. Macedonioab, Francesca, Aamer Alia, Teresa Poerioa, Essam El-Sayed, Enrico Drioliabd, and Mahmoud Abdel-Jawadc, *Direct contact membrane distillation for treatment of oilfield produced water.* Separation and Purification Technology, 2014. **126**: p. 69-81.
34. Curcio, Efrem and Enrico Drioli, *Membrane Distillation and Related Operations—A Review.* Separation & Purification Reviews 2005. **34**(1).
35. Drioli, Enrico, Aamer Ali, and Francesca Macedonio, *Membrane distillation: Recent developments and perspectives.* Desalination, 2015. **356**: p. 56-84.
36. Said, Ibrahim A., Sen Wang, and Qilin Li, *Field Demonstration Of A Nanophotonics Enabled Solar Membrane Distillation Reactor For Desalination.* Industrial & Engineering Chemistry Research, 2019. **58**(40): p. 18829-18835.
37. Kellogg, Bernard, *Development and Evaluation of Electrospun Nanocomposite Coatings for Solar Membrane Distillation*, in *Civil and Environmental Engineering*. 2018, Rice University: Rice University.
38. Wu, K. R. Zodrow, P. B. Szemraj, and Q. Li, *Photothermal nanocomposite membranes for direct solar membrane distillation.* Journal of Materials Chemistry A, 2017. **5**: p. 23712-23719.
39. A.Said, Ibrahim, Timothy R.Chomiak, Ze He, and Qilin Li, *Low-Cost High-Efficiency Solar Membrane Distillation For Treatment of Oil Produced Waters.* Separation and Purification Technology, 2020. **https://doi.org/10.1016/j.seppur.2020.117170**.

40. Said, Ibrahim A, Tim Chomiak, John Floyd, and Qilin Li, *Sweeping Gas Membrane Distillation (SGMD) for Wastewater Treatment, Concentration, and Desalination: A Comprehensive Review.* Chemical Engineering & Processing: Process Intensification, 2020. **153**(107960) https://doi.org/10.1016/j.cep.2020.107960.
41. Shahua, Vandita T. and S. B. Thombre, *Air gap membrane distillation: A review.* Journal of Renewable and Sustainable Energy, 2019. **11**(4): p. 045901.
42. Arkema, *Plexiglas Acrylic Sheet: Optical & Transmission Characteristics*. 2000: Philadelphia, PA. p. 1-12.
43. Dongare, Pratiksha D., et al. , *Solar thermal desalination as a nonlinear optical process.* PNAS, 2019. **116**(27): p. 13182-13187.